Università degli Studi di Ferrara

DOTTORATO DI RICERCA IN
"Medicina Molecolare e Farmacologia"

CICLO XXIX

COORDINATORE Prof. Francesco Di Virgilio

Kevetrin: preclinical study of activity and molecular mechanisms of a new promising molecule in Acute Myeloid Leukemia

Settore Scientifico Disciplinare MED/15

Dottorando
Dott. Napolitano Roberta

Tutore
Prof. Cuneo Antonio

Co-Tutore
Dott. Calistri Daniele

Anni 2014/2016

INTRODUCTION

1. ACUTE MYELOID LEUKEMIA

Acute Myeloid Leukemia (AML) is a heterogeneous disorder defined by clonal expansion of immature myeloid cells (blasts) that infiltrate peripheral blood, bone marrow and other tissues (1)(2). Worldwide, it is the most common myeloid leukemia, with a median age at diagnosis of around 70 years (3) and it is curable in 35-40% of 60 years old patients and in 5-15% of those who are older than 60 (4).

1.1 Classification

In 1970 a French-American-British (FAB) co-operative group proposed, for the first time, a uniform system of classification and nomenclature of acute myeloid leukemias, based on morphology and immune-phenotype/cytochemical criteria, defining eight major AML subtypes (FAB M0 to M7)(Figure 1) (5).

FAB subtype	Description	Comments
M0	Undifferentiated	Myeloperoxidase negative; myeloid markers positive
M1	Myeloblastic without maturation	Some evidence of granulocytic differentiation
M2	Myeloblastic with maturation	Maturation at or beyond the promyelocytic stage of differentiation; can be divided into those with t(8;21) AML1–ETO fusion and those without
M3	Promyelocytic	APL; most cases have t(15;17) PML–RARα or another translocation involving RARα
M4	Myelomonocytic	
$M4_{Eo}$	Myelomonocytic with bone-marrow eosinophilia	Characterized by inversion of chomosome 16 involving CBFβ, which normally forms a heterodimer with AML1
M5	Monocytic	
M6	Erythroleukaemia	
M7	Megakaryoblastic	GATA1 mutations in those associated with Down's syndrome

AML1, acute myeloid leukaemia 1; APL, acute promyelocytic leukaemia; PML, promyelocytic leukaemia; RARα, retinoic-acid receptor-α. Modified from REF. 65.

Figure 1. **FAB classification of AML (6).**

In 2008 the World Health Organization (WHO) replaced the FAB classification system, defining seven AML subtypes: AML with recurrent genetic abnormalities, AML with myelodysplasia related changes, therapy-related myeloid neoplasms, AML not otherwise specified (NOS), myeloid sarcoma, myeloid proliferations related to Down syndrome and blastic plasmocytoid dendritic cell neoplasms (1). WHO classification's last update was done in 2016 providing few changes to the existing categories (Figure 2) (4).

Figure 2. WHO classification of AML (4).

1.2 Morphology

AML blasts present different sizes, a reduced cytoplasm and a larger nucleus, containing several nucleoli. On their surface blasts can expose common differentiation (CD) markers usually expressed by healthy immature myeloid cells like CD13, CD33 or CD34 (7). Depending on the morphological subtype and the differentiation status they can present, also, monocytic differentiation (CD4, CD14 and CD11b), megakaryocytes (CD14a and CD61) or erythroid (CD36 and CD71) markers. In some cases both T and B cell lineages

antigens are co-expressed, defining a mixed phenotypic leukemia with a worse overall survival (Figure 3) (8).

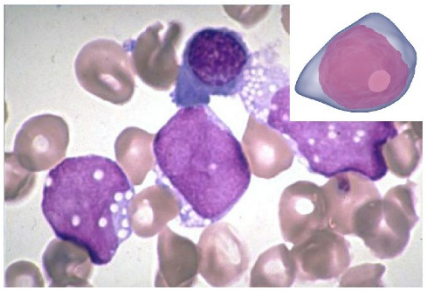

M0 Acute myeloblastic leukaemia with minimal differentiation

Morphology:

Can resemble LLA-L2 blasts. Medium-sized blasts, rounded nucleus, fine chromatin, basophilic non-granular cytoplasm, prominent nucleoli.

Immunophenotype

- CD13 +
- CD33 +
- CD11b +
- CD11c +
- CD14 +
- CD15 +

Photo courtesy of: Acute myeloid leukemia pathophysiology, 2012

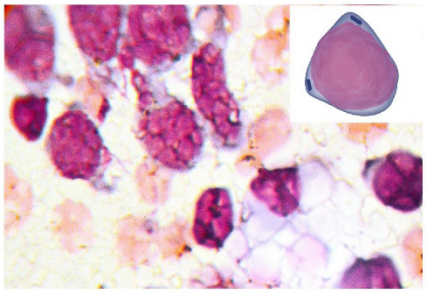

M1 Acute myeloblastic leukaemia without maturation

Morphology:

Medium-sized blasts with high nucleo:cytoplasm (n:c) ratio, rounded nuclei with immature, dispersed chromatin with one or more prominent nucleoli. Blasts can show fine azurophilic granulation or isolated Auer rods in the cytoplasm in 5% to 10% of cases

Immunophenotype

- MPO +
- CD13 +
- CD33 +
- CD117+
- CD34 +/-

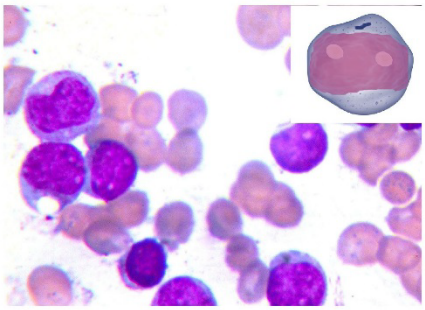

M2 Acute myeloblastic leukaemia with maturation

Morphology:

Small to medium-sized blasts with high nucleo: cytoplasm (n:c) ratio and rounded nuclei sometimes located in a corner of the cytoplasm. The nucleus shows dispersed, immature chromatin with one or more nucleoli. The cytoplasm is basophilic and can contain traces of primary azurophilic granulation or isolated Auer rods.

Immunophenotype

- MPO +
- CD34 +/-
- CD13 +
- CD15 +
- HLA-DR +/-
- Sudan black +
- CD117 +/-

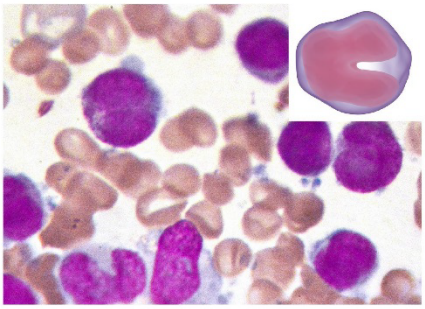

M3 Promyelocytic leukaemia

Morphology:

Abundant, intensely azurophilic granulation. The nucleus is usually monocytic in appearance (reniform) and is either irregular or bilobed with a deep cleft. Scarcely basophilic cytoplasm due to the proliferation of azurophilic granulation. Some atypical promyelocytes also contain elongated or splinter-shaped crystalline cytoplasmic inclusions specific to this type of leukaemia.These usually form clumps, but differ from Auer rods in that they show a tubular substructure on electronic microscopy.

Immunophenotype

- CD13 +
- CD33 +
- HLA-DR -
- CD34 -

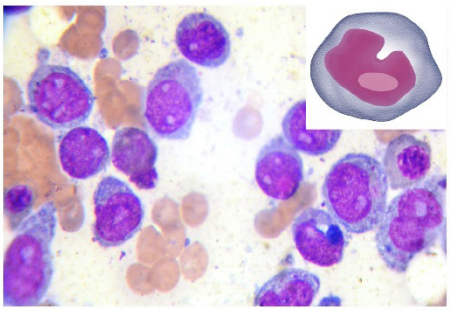

M4 — Acute myelomonocytic leukaemia

Morphology:

Large blasts, moderate nucleo:cytoplasm (n:c) ratio and variable basophilia. The nucleus may be rounded, kidney-shaped or irregular. Nucleoli are usually prominent.

Immunophenotype

- CD13 +
- CD15 +
- CD33 +
- CD11b +
- CD11c +
- CD14 +
- CD64 +
- CD4 +

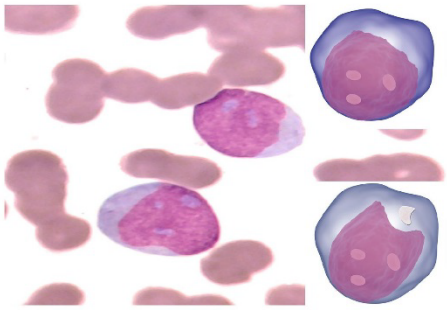

M5 — Acute monocytic leukaemia

M5a acute monoblastic leukaemia:
Large blasts with rounded nucleus and dispersed, immature chromatin (1-3 nucleoli) and moderately large and intensely basophilic cytoplasm. The cytoplasm may show some Auer rods and/or prolongations and granulations.
M5b acute monocytic leukaemia
Promonocytes have a rounded or kidney-shaped nucleus with a less basophilic cytoplasm that is more highly granulated than monoblasts and contains some vacuoles. A findings of erythrophagocytosis together with monocytic blasts suggests a t(8;16) translocation.

Immunophenotype

- CD14 +
- CD68 +
- CD4 +
- CD11c +
- HLA-DR +
- CD64 +

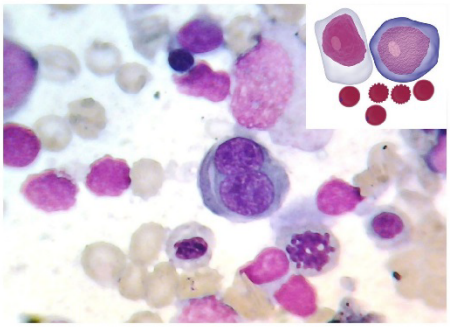

M6 — Acute erythroid leukaemia

M6a erythroid leukaemia with proliferation of mixed blasts:
Over 50% erythroid precursors and around 30% myeloblasts. Morphology of erythrocytes in peripheral blood is greatly changed, with schistocytes, "pincered" or mushroom-shaped cells, and spiculated echinocyte and acanthocyte cells.
M6b pure erythroid leukaemia:
Erythroids make up 80% of bone marrow cells, with less than 3% myeloid cells. Erythrocytes in peripheral blood consist of macrocytes, basophilic stippling, Howell-Jolly bodies or Cabot rings.

Immunophenotype

- CD13 +
- CD33 +
- CD15 +
- Glycophorin A +
- Glycophorin C +

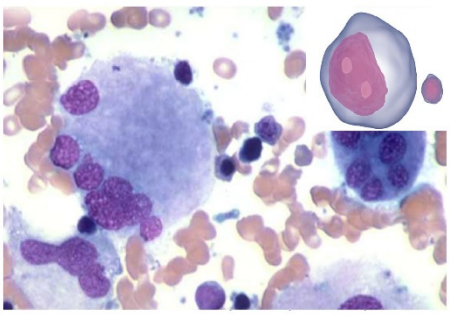

M7 — Acute megakaryocytic leukaemia

Morphology:

Highly immature, polymorphic blasts. The nucleus is eccentric with dispersed, reticulated chromatin and 1-3 prominent nucleoli. The cytoplasm is non-granular, basophilic, and very similar in appearance to platelets, with pseudopods or granulations. Micromegakaryocytes and fragments of megakarioblasts are seen in peripheral blood (giant platelets, some highly degranulated).

Immunophenotype

- CD41 +
- CD61 +
- CD42 +
- CD13 +
- CD33 +
- CD34 +

Figure 3. FAB classification: morphology and immunophenotype of AML subtypes (9).

1.3 Cytogenetics

AML are often characterized by non-random chromosomal abnormalities that have long been recognized as the cause of disease development and progression (10). The advent of next-generation sequencing has provided a better knowledge of AML genetic landscape, identifying several key molecular abnormalities, now used for predicting outcome and supporting the choice of treatment strategy. In 2013 the Cancer Genome Atlas Research Network analyzed the genome of 200 adult AML cases, founding 23 significantly mutated genes that were organized into eight functional categories (Figure 5) (11)(2):

1. **Signaling genes**, as the Fms Related Tyrosine Kinase gene 3 (*FLT3*), that confers a proliferative advantage, acting on different important signaling pathways like RAS-RAF, JAK-STAT and PI3K-AKT. Around 20% of all AML cases show internal tandem duplications, in the juxta-membrane domain, or mutations, in the tyrosine kinase domain, of the *FLT3* gene, activating its signaling and promoting tumor proliferation (12)(13).

2. **Myeloid Transcription Factor genes**, as the Runt-related Transcription Factor 1 (*RUNX1*), also known as Acute Myeloid Leukemia 1 (*AML1*), that physiologically activates C/EBPα, promoting the transcription of its regulated genes (6). *RUNX1* is located at chromosome 21q22 and, in M2 AML subtype, it is frequently translocated with the Eight Twenty One (*ETO*) gene, or *RUNX1T1*, located at chromosome 8q22 (14). This translocation generates a fusion protein, AML-ETO, that binds the AML1 site, inhibiting C/EBPα activation by the recruitment of corepressors (Figure 4) (6).

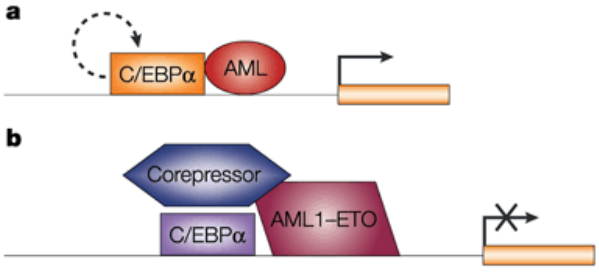

Figure 4. AML-ETO fusion protein (6).

3. **Nucleophosmin gene (*NPM1*)**, encoding a nucleo-cytoplasmic shuttling protein, is the most frequent mutated gene in AML. *NPM1* mutations result in the aberrant

cytoplasmic localization of the related protein, leading to myeloid proliferation and leukemia development (15).

4. **Spliceosome-complex genes**, such as Serine and arginine Rich Splicing Factor 2 (*SRSF2*), Splicing factor 3B subunit 1 (*SF3B1*) and U2 Small Nuclear RNA Auxiliary Factor 1 (*U2AF1*), fundamental in the regulation of RNA processing. Mutations of splicing factor genes have been associated with the development of Myelodysplastic Syndromes (16).

5. **Cohesin-complex genes**, as Stromal Antigen 2 (*STAG2*) and double-strand-break repair protein (*RAD21*), important in transcriptional regulation, DNA-loop formation and chromosome segregation.

6. **Genes involved in chromatin modification**, as Additional sex comb-like 1 (*ASXL1*) and Enhancer of zeste homolog 2 (*EZH2*), related to chromatin modification, as well as Histone-lysine N-methyltransferase 2A (*KMT2A*) - myeloid/lymphoid leukemia translocated to 3 (*MLLT3*) fusion gene, originated by the translocation t(9;11)(p22;q23).

7. **Genes involved in DNA Metilation**, such as DNA methyltransferase 3A (*DNMT3A*), Ten-Eleven Translocation 2 (*TET2*) and Isocitrate Dehydrogenases (*IDH 1* and *2*).

8. **Tumor-suppressor genes**, such as *TP53*, mutated in 8%-14% of AML cases. *TP53* mutations are commonly associated with a complex karyotype and confer a very adverse prognosis with chemoresistance (17).

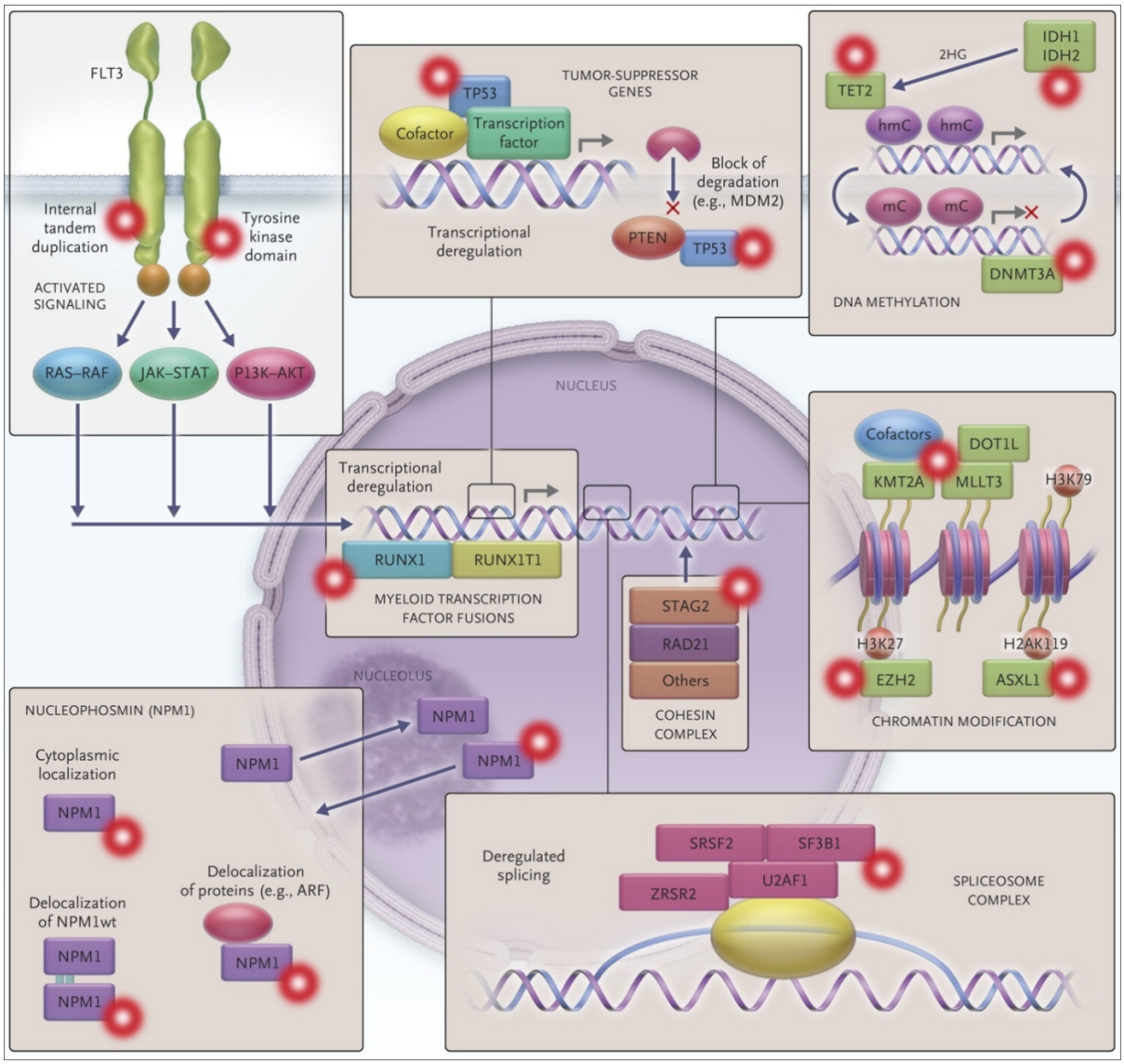

Figure 5. Functional categories of genes commonly mutated in AML (2).

Another important cytogenetic alteration, characterizing M3 AML subtype, is the translocation t(15;17). This translocation lead to the fusion of the Retinoic Acid Receptor α (*RARα*) gene, located at 17q21, with the Promyelocitic Leukemia gene (*PML*), located at 15q22, creating a fusion protein, PML–RARα, that induces a maturation block at the promyelocytic level (18).

Depending on molecular and cytogenetic alterations and according to the European LeukemiaNet recommendations, AML patients can be classified into four risk groups (Figure 6) (19):

1. **Favorable**, that includes acute promyelocytic leukemia, balanced abnormalities, nucleophosmin gene mutations that aren't associated with internal tandem duplication mutations in *FLT3* (*FLT3*-ITD) and *CEPBA* biallelic mutations.
2. **Intermediate 1**, that includes AML cases with a normal karyotype, excluding those included in the previous group.
3. **Intermediate 2**, defined by patients with *MLLT3-KMT2A* fusion gene and AML cases with cytogenetic abnormalities neither favorable nor adverse.
4. **Adverse**, that includes the remaining chromosomal abnormalities and patients with a complex karyotype, identified by three or more chromosomal alterations without, at least, one of the WHO-designed recurring translocations or inversions. Usually patients with a complex karyotype present also a mutation or a deletion of the *TP53* gene.

Risk Profile	Subsets
Favorable	t(8;21)(q22;q22); *RUNX1-RUNX1T1* inv(16)(p13.1q22) or t(16;16)(p13.1;q22); *CBFB-MYH11* Mutated *NPM1* without *FLT3*-ITD (normal karyotype) Biallelic mutated *CEBPA* (normal karyotype)
Intermediate-I†	Mutated *NPM1* and *FLT3*-ITD (normal karyotype) Wild-type *NPM1* and *FLT3*-ITD (normal karyotype) Wild-type *NPM1* without *FLT3*-ITD (normal karyotype)
Intermediate-II	t(9;11)(p22;q23); *MLLT3-KMT2A* Cytogenetic abnormalities not classified as favorable or adverse‡
Adverse	inv(3)(q21q26.2) or t(3;3)(q21;q26.2); *GATA2–MECOM (EVI1)* t(6;9)(p23;q34); *DEK-NUP214* t(v;11)(v;q23); *KMT2A* rearranged –5 or del(5q); –7; abnl(17p); complex karyotype§

Figure 6. Current ELN risk stratification of molecular and cytogenetic alterations in AML (19).

1.4 AML treatment

Over the past 30 years the therapeutic strategy designed for AML patients remains unchanged and it is composed by an initial intensive induction therapy followed by a consolidation therapy, as a post-remission strategy (4). The induction therapy actually is composed by an anthracycline, that is added to the cytarabine continuous-infusion. Using this therapy 60-85% of patients, who have 60 years of age or younger, achieve complete remission. Patients older than 60 present a lower rate of complete response (from 40 to 60%). Once achieved complete remission the goal of consolidation strategies is to prevent relapse and eradicate the minimal residual disease. Conventional post-remission strategies

include chemotherapy, such as intermediate-dose cytarabine, for patients with favorable genetic risk, or allogeneic hematopoietic-cell transplantation, for patients associated to the other three risk categories. For Acute Promyelocytic Leukemia patients, the treatment with all-trans retinoic acid (ATRA), represents the standard of care (2).

Several new compound have been studied for improving AML therapeutic alternatives. Some of these new molecules have been developed starting from frequent molecular alterations, such as Tyrosine Kinase (20) or IDH inhibitors (21). Other studies were focused on hypomethylating agents (22) or immune therapies (23). Nowadays, after a more complete understanding of AML molecular pathogenesis, a lot have to be done for using this knowledge into clinical practice in order to develop new therapeutic alternatives for this disease.

2. Tumor Protein 53

TP53 is a 20.000 bp gene, located on the short arm of chromosome 17 (17p13). *TP53* gene mutations are reported in the majority of tumors and the most frequent mutation is a single monoallelic missense mutation (74%), that originates a stable full-length protein (24). Human *TP53* gene is composed by 11 exsons and encodes a 53 kDa protein, defined by five domains (Figure 7) (25):

1. **The amino-terminal domain** (aa 1-42), that contains the transactivation domain, which is responsible for the activation of downstream p53 target proteins.
2. **The proline-rich domain** (aa 40-92), that mediates p53 response to DNA damage.
3. **The DNA-binding domain** (aa 101-306), which contains the DNA binding site and is the target of 90% of *TP53* mutations in human cancers, inhibiting protein's DNA-binding activity (26).
4. **The oligomerization domain** (aa 307-355), that consists of a β-strand, which interacts with another p53 monomer to form a dimer, followed by a α-helix which mediates the dimerization of p53 dimers to form a tetramer.
5. **The carboxy-terminal domain** (aa 356-393), that presents several nuclear localization sequences (NLS).

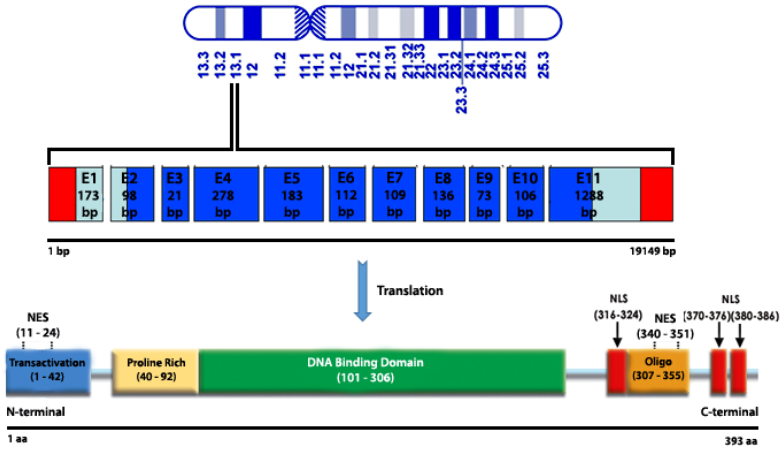

Figure 7. TP53 gene and protein structure (25).

p53 has a key role in the regulation of cellular response to stress signals as DNA damage, hypoxia and hyperproliferation (27). Once activated p53 can migrate into the nucleus, promoting the expression of several genes involved in cell growth arrest, such as protein 21 (*p21*), apoptosis, as bcl-2-like protein 4 (*BAX*) or p53 upregulated modulator of apoptosis (*PUMA*), and DNA repair, such as the Growth Arrest and DNA Damage protein (*GADD45*). Moreover, p53 regulates genes involved in its own turnover and activity as E3 ubiquitin ligase mouse double minute 2 (*MDM2*) (28)(29). In normal conditions, p53 is maintained at a low level and its rapid turnover is associated to a correct folding by chaperon proteins, such as Hsp90 (30) and is mainly regulated by MDM2, which ubiquitinates the protein, promoting its proteasomal degradation (31). MDM2 can also shuttle p53 out of the nucleus (31)(32) and prevent its interaction with transcriptional co-activators (33). Under stress conditions p53 is phosphorylated, mainly at serine 15 and 20, by various sensor kinases, as ataxia-telangiectasia mutated kinase (ATM), promoting the dissociation of p53-MDM2 complex and protein stabilization and activation (Figure 8) (34)(35)(36)(37)(38).

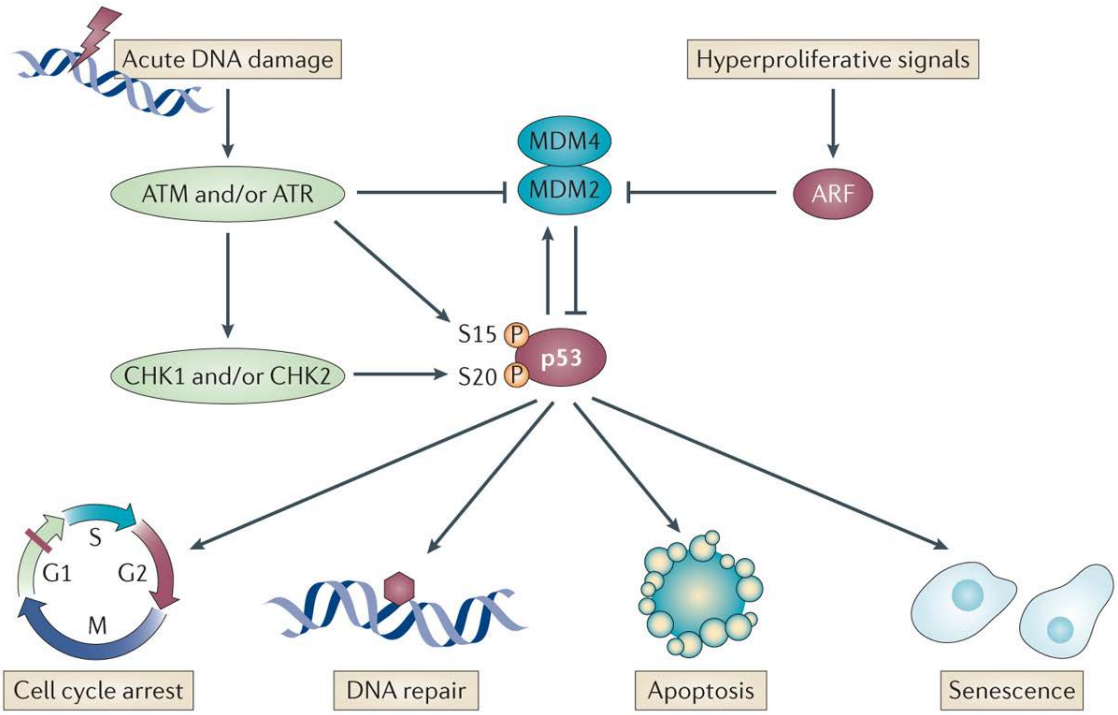

Figure 8. p53 activation and response (38).

p53 can also interact with other important factors, such as the NAD-dependent protein deacetylase Sirtuin 3 (SIRT-3). SIRT-3 appears, indeed, coupled with p53 during its initial expression, usually by inhibiting p53 activity to induce growth arrest. Li et al. recently showed how, in bladder cancer, p53 can be deacetylated by SIRT-3, partially abrogating p53 activity to induce growth arrest (39)(40).

3. KEVETRIN

Kevetrin is a new molecule compound, produced by Cellceutix (41), that is water-soluble and non-genotoxic (Figure 9). It has a 30 minutes half life and a 150-250 μM peak plasma concentration.

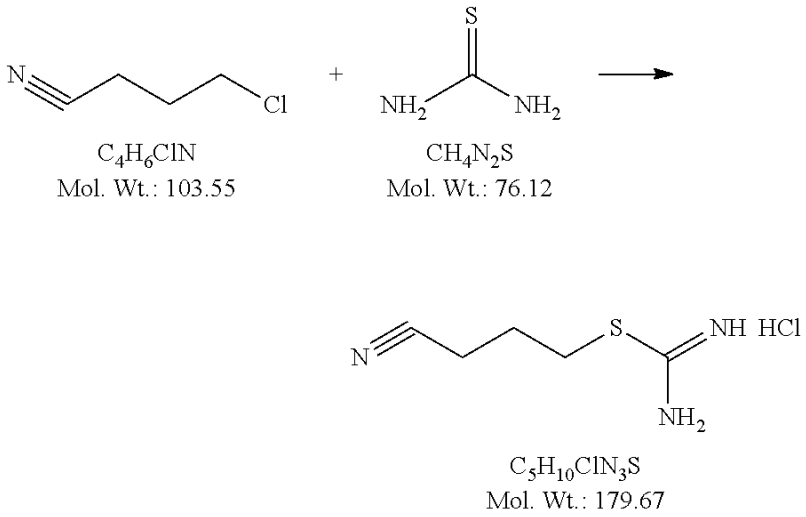

Figure 9. Kevetrin chemical structure (41).

At first, it was classified as an alkylating agent and a Protein kinase B (AKT) inhibitor (42), with anti-angiogenic properties. Experiments realized using several cancer models revealed a great activity of the molecule in those cancers types characterized by the p53 protein expression. Moreover, the loss of p53 functionality influenced only marginally the cytotoxicity of Kevetrin. The role of p53 in Kevetrin's activity was further investigated, revealing a dual mechanism of action of the molecule, depending on *TP53* mutational status (43)(44):

- in ***TP53* wild type** models, Kevetrin was able to induce cell cycle arrest and apoptosis through the activation and stabilization of wild type p53, resulting in an increased expression of p53 target proteins, p21 and PUMA (45).

- in ***TP53* mutated** models, oncogenic mutant p53 is normally complexed with Hsp90, which is highly up-regulated in several malignancies (46)(47)(48), including hematological ones, as AML (49), and its over-expression is related to histone deacetylase 6 (HDAC6) positive regulation. Kevetrin was able to induce

HDAC6 down-regulation, negatively affecting Hsp90 expression levels and promoting the mutated form's degradation, with apoptosis induction (50).

Kevetrin has been extensively studied, *in vivo* and *in vitro*, in several cancer models, such as lung, breast, colon and ovarian cancer (45)(50). Up to now Cellceutix successfully completed the first Phase-I clinical trial evaluating Kevetrin's activity in Advanced Solid Tumors, with patients showing good toleration and signs of a potential therapeutic response (NCT01664000) (51)(52). A Phase-IIa trial will start in Platinum-Resistant Ovarian Cancer. Recently, Kevetrin has also be awarded, by the Food and Drug Administration, the Orphan Drug status for Ovarian Cancer, Pancreatic Cancer, and Retinoblastoma (44).

AIM OF THE PROJECT

Acute Myeloid Leukemia (AML) is the most common leukemia and it is characterized by blasts clonal expansion and peripheral blood and bone marrow infiltration (2).
AML therapeutic strategies remain unchanged since 1970 (4) and the majority of patients often eventually relapse and die due to disease progression (1).
TP53 transcription factor is a key regulator of several cellular pathways, such as DNA repair, cell cycle, apoptosis and angiogenesis (53). It is mutated in 8-14% of AML cases and its mutations are commonly associated with a complex karyotype, conferring a very adverse prognosis (17).
Kevetrin is a new emerging drug with the ability to target both wild type and mutant p53 tumors, promoting apoptosis (45)(50).

The main aim of this project is to explore cellular and molecular alterations induced by Kevetrin, focusing on its role in the p53 pathway.
The secondary objective is to clarify if Kevetrin may represent a promising therapeutic strategy in AML treatment.

For these reasons, several cellular and molecular assays have been performed on two AML cell lines characterized by different *TP53* mutational status and cytogenetic characteristics.

MATERIALS and METHODS

1. CELL LINES

Acute myeloid leukemia cell lines, MOLM-13 (AML M5) and KASUMI-1 (AML M2), were obtained from the American Type Culture Collection (ATCC, Rockville, MD). Cell lines were cultured at 37°C in a 5% CO_2 atmosphere, maintaining a density of 300.000 cells/ml. The culture medium was composed by RPMI 1640 (Euroclone, Milan, Italy) supplemented with 20% heat inactivated fetal bovine serum (GE Healthcare, Piscataway, NJ), 2 mM L-glutamine (GE Healthcare), 100 U/ml penicillin and 100 μg/ml streptomycin (GE Healthcare) and 0.2% Mycozap (Lonza, Walkersville, MD). For all the experiments cells were used in the exponential growth phase.

2. DRUG

Kevetrin powder was kindly provided by Cellceutix (Beverly, Massachusetts, USA), dissolved in sterile water in a 600 μg/ml stock solution and stored at 4°C. The drug was diluted in medium immediately before use and tested in a concentration range of 15 – 60 μg/ml.

3. TP53 MUTATION ANALYSIS

DNA was extracted from cell lines using QIAamp DNA Mini kit (Qiagen, Hilden, Germany) in accordance with the manufacturer's instructions. DNA quantity and quality were assessed by Nanodrop (Celbio, Milan, Italy). Starting from 50 nanograms of DNA, *TP53* exons 5, 6, 7, 8 were amplified by Polymerase Chain Reaction and analyzed by Direct Sequencing using 3130 Genetic Analyzer (Applied Biosystems, Foster City, CA, USA).

4. CELL VIABILITY ASSAY

Cell viability was determined using CellTiter 96® AQueous One Solution Cell Proliferation Assay, based on 3-(4,5-dimethylthiazol-2-yl)-5-(3-carboxymethoxyphenyl)-2-(4-sulfophenyl)-2H-tetrazolium inner salt (MTS) (Promega, Wisconsin, USA). Cells were seeded in 100μl of culture medium and, after the treatment, 20μl of Solution Reagent were added into each well of the 96-well assay plate. Cells were incubated for 3 hours (h) at 37°C and 5% CO_2. The optic density (OD) was determined at a wavelength of 490 nm by

THERMO MULTISKAN EX microplate reader (Thermo Fisher Scientific, Massachusetts, USA).

5. FLOW CYTOMETRY

Flow cytometric analysis were performed using a FACSCanto flow cytometer (Becton Dickinson, San Diego, CA, USA) equipped with 488 nm (blue) and 633 (red) lasers and 10,000 events were recorded for each sample. Data acquisition and analysis were performed using FACSDiva (Becton Dickinson).

5.1 Annexin V assay

Cells were washed once in phosphate buffered saline (PBS) and incubated with 25μl/ml of Annexin V-fluorescein isothiocyanate (FITC) in binding buffer (eBioscence, San Diego, CA) for 15 minutes (min) at 37°C in a humidified atmosphere in the dark. Cells were washed in PBS and re-suspended in binding buffer. Before flow cytometric analysis, propidium iodide (PI) was added to a final concentration of 5 μg/ml.

5.2 Tunel assay

Fragmented DNA was detected by the terminal deoxynucleotidyl transferase (TdT) nick-end labeling (TUNEL) assay. After each treatment, cells were washed with PBS, fixed in 1% Formaldehyde on ice for 15 min, suspended in 70% ice-cold ethanol and stored overnight (o/n) at -20°C. Cells were, then, washed in PBS and incubated 5 min at 4°C in PBS containing 0.1% Triton X-100 (Bio-Rad, Hercules, CA). Thereafter, samples were incubated in 50 μl of solution containing TdT and FITC conjugated dUTP deoxynucleotides 1:1 (Roche Diagnostics GmbH, Mannheim, Germany) and incubated 90 min at 37°C in a humidified atmosphere in the dark. Samples were washed in PBS, counterstained with 2.5 mg/ml propidium iodide (MP Biomedicals, Verona, Italy) and 10 kU/ml RNAse (Sigma-Aldrich, St. Louis, MO) for 120 min at 4°C in the dark and analyzed by flow cytometry.

5.3 Mitochondrial Membrane Potential Depolarization Analysis (ΔΨm)

Cells were washed once in PBS and incubated in JC-1 Working solution (BD Biosciences Pharmingen, San Diego, CA) for 15 min in a humidified atmosphere at 37°C in the dark, according to manufacturer's instructions. Cells were then washed twice, suspended in 1X Assay Buffer (BD Biosciences) and analyzed by flow cytometry.

5.4 Cell Cycle

After the treatment, cells were washed in PBS 1X, fixed in 70% ice-cold ethanol, stained with 10 mg/ml propidium iodide (MP Biomedicals), 10 kU/ml RNAse (Sigma Aldrich) and 0.01% NP40 (Sigma Aldrich) o/n at 4°C in the dark and analyzed by flow cytometry. Data analysis were performed using ModFit 2.0 (DNA Modelling System, Verity Software House, Inc., Topsham, ME, USA).

5.5 Active Caspase-3 Assay

The percentage of active Caspase-3 was measured using the FITC Active Caspase-3 Apoptosis Kit (BD Biosciences). After the treatment, cells were collected, washed twice with ice-cold PBS, and incubated 20 min at 4°C in BD Cytofix/Cytoperm (BD Biosciences). Samples were washed with BD Perm/Wash™ buffer 1X (BD Biosciences) and incubated with 20 μl of Rabbit Anti-Active Caspase-3 (BD Biosciences) for 30 min at room temperature (RT) in the dark. Each sample was washed in BD Perm/Wash™ buffer and analyzed by flow cytometry. A positive control for each experiment was used.

6. IMMUNOFLUORESCENCE

After the treatment, cells were seeded in 6 wells and cultured in a humidified CO2 atmosphere for 24 and 48 h. After the count 500.000 cells were fixed in 4% (v/v) Formaldehyde for 15 min, blocked for 60 min at RT with a 5% BSA, 0.3% Triton X-100 solution (Sigma-Aldrich) and incubated o/n at 4°C with a rabbit monoclonal anti-human p53 antibody (Cell Signaling Technology, Inc., Danvers, MA, USA), used at a dilution of 1:1000. The day after, samples were washed with PBS, incubated with a Phycoetythrine-conjugated anti-rabbit secondary antibody (Invitrogen, Carlsbad, CA) for 1 h at RT and rinsed in PBS. Cells were, then, cytospinned 5 min at 800 rpm on positive-charged slides (Bio Optica, Milan, Italy). Slides were mounted with Slowfade Diamond Antifade Mountant with DAPI (Invitrogen) and staining was evaluated using a fluorescent microscope (Axioscope; Zeiss, Göttingen, Germany). Controls for each experiment were used.

7. WESTERN BLOT

Total protein extracts were prepared in ice-cold lysis buffer (0.5% Nonidet P-40 [NP-40], 250 mM sodium chloride [NaCl], 50 mM N-2-hydroxyethylpiperazine-N'-2-ethanesulfonic acid [Hepes], 5 mM ethylenediaminetetraacetic acid [EDTA], and 0.5 mM ethyleneglycol bis (beta-aminoethylether)-N,N,N',N tetraacetic acid [EGTA]) containing phosphatase inhibitor cocktail 2 (Sigma-Aldrich), protease inhibitor (Clontech, Mountain View, CA), and dithiothreitol (DTT) (Invitrogen). Proteins were collected 48 h after the treatment at different concentrations (15-30-60 μg/ml). BCA protein assay kit (Pierce, Rockford, IL) was used to measure protein concentration. Proteins were separated by polyacrylamide gel (Bio-Rad) electrophoresis and were transferred to 0.2 μm nitrocellulose membranes (Bio-Rad). The following antibodies were used: anti-HSP90AB1 (clone 4C10, 1:2000) from Origene, anti-p53 (clone 7F5, 1:1000), anti-SIRT-3 (clone C73E3, 1:1000), anti-Phospho-p53 (Ser15) (clone 16G8, 1:1000), anti-p21 (clone DCS60, 1:2000) and anti-PUMA (clone D30C10, 1:1000) all from Cell Signaling. Proteins were detected by chemiluminescence. Anti-β-actin (clone AC-15, 1:50000) from Abcam and Anti-vinculin (1:1000) from Invitrogen were used as normalizer. Quantitative analysis was carried out with QuantityOne Software.

8. GENE EXPRESSION PROFILING (GEP)

RNA was isolated using TRIzol (Invitrogen) from no drug controls and samples treated with Kevetrin 60 μg/ml. Labeled ss-cDNA was prepared from 100 ng RNA and hybridized to Human Transcriptome Array 2.0 (Affymetrix, Santa Clara, California, USA) according to the manufacturer's recommendations. Three independent samples of each condition per cell line were analyzed. Data quality control and normalization, and supervised analysis were performed using Expression Console and Transcriptome Analysis Console softwares, respectively (Affymetrix).

9. STATISTICAL ANALYSIS

All experiments were performed at least three times. Quantifiable data were derived from three independent experiments. Statistical analysis was carried out using GRAPH PAD PRISM 5.0 software by applying the Student t test for 2-group comparisons. Differences were considered significant at $p < 0.05$.

RESULTS

1. BACKGROUND

The initial aim of my research project was to evaluate the effect of innovative compounds, in classical Hodgkin Lymphoma (cHL) cell lines, as new promising therapeutic strategies. At first, we focused on Kevetrin, a new drug with a different mechanism of action depending on *TP53* mutational status (wild type or mutated). Sequencing cHL cell lines (HDLM2, L-428, L-1236), we found that all the chosen models were characterized by *TP53* gene deletions. In order to better understand drug's activity, we performed some preliminary experiments on two acute myeloid leukemia (AML) cell lines with a more defined *TP53* mutational status: KASUMI-1, a *TP53* mutated cell line (characterized by a homozygous point mutation), and MOLM-13, a wild type model. Starting from the results obtained in AML, we noticed a more selective action of the drug for the mutated cell line and we decided to deep investigate Kevetrin's mechanism of action in this model. We were also supported on this way by the developing, at the Hematology institute of Bologna, of a Phase-II study protocol involving Kevetrin as a single agent or in combination with Cytarabine in Acute Myeloid Leukemia patients. Starting from the study design and encouraged by the inventor of the molecule, at first we tested a pulsed treatment, in order to use an *in vitro* treatment as similar as possible to the clinical schedule, characterized by 6 hour infusion every two-three days in a four week cycle. Unfortunately, the pulsed treatment didn't show a clear effect. We, therefore, decided to move to a continued treatment, in order to clarify drug's mechanism of action in our model.

2. CELL LINES CHARACTERIZATION

At first, we verified the mutational status of the *TP53* gene in the selected cell lines, in order to confirm the one described by the literature. We sequenced *TP53* gene from exon 5 to exon 8 and, for MOLM-13 cell line, we confirmed a wild type status of the *TP53* gene; for KASUMI-1 we found the described homozygous point mutation of Exon 7, associated to a substitution of Arginine (R) with Glutamine (Q), changing residue's polarity and creating a disruptive mutation, with a non-functional protein (Table 1).

AML cell lines	*TP53* status from literature	*TP53* ex5	*TP53* ex6	*TP53* ex7	*TP53* ex8
KASUMI -1 (AML-M2)	***TP53* mutated** Homozygous point mutation of Exon 7	**WT**	**WT**	**R248Q cod248 CGG-->CAG**	**WT**
MOLM – 13 (AML-M5)	***TP53* wt**	**WT**	**WT**	**WT**	**WT**

Table 1. *TP53* mutational status of AML cell lines.

3. PULSED TREATMENT

The first schedule we tested was associated to a pulsed treatment, characterized by 6 hour treatment plus a wash out (wo) of 66 hours (h) in a two week cycle with three pulsations every treatment (Figure 10).

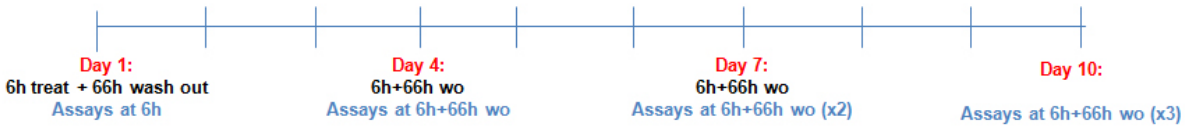

Figure 10. Pulsed treatment schedule.

3.1 KEVETRIN INDUCES A DECREASE OF VIABILITY IN KASUMI-1 CELL LINE

To investigate the response of AML cell lines to Kevetrin, we evaluated KASUMI-1 and MOLM-13 cell viability using the MTS assay after exposure to different concentrations of Kevetrin (15, 30 and 60 µg/ml) for 6h, 6h+66h wo, 6h+66h wo (x2) and 6h+66h wo (x3). As visible in Figure 11, the two cell lines showed different outlines: the mutated one (KASUMI-1), showed a dose and time-dependent inhibition of cell viability with IC50 at 6h+66h wo (x2) of 53 µg/ml; on the other side, the wild type cell line (MOLM-13) didn't show any inhibition of cell viability.

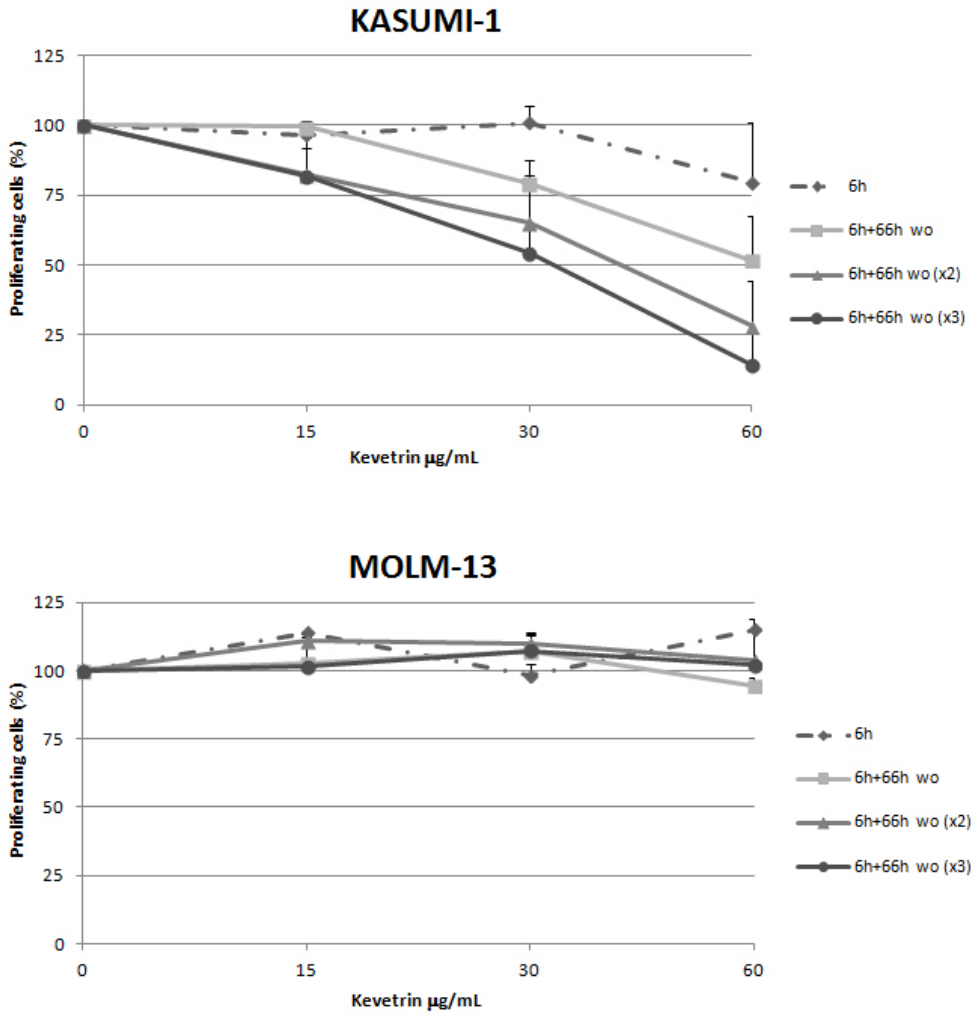

Figure 11. Kevetrin effect on AML cell lines proliferation.

Survival curve of AML cell lines treated with different concentrations of Kevetrin (15 – 30 – 60 µg/ml) for up to three pulsations. Values represent the mean ± SD of three independent experiments in triplicate.

3.2 KEVETRIN INDUCES A SLIGHT APOPTOSIS INCREASE IN KASUMI-1 CELL LINE

To investigate the role of apoptosis into Kevetrin's effect in our models, we examined phosphatidylserine externalization, DNA fragmentation and Caspase-3 activation in cells treated with 60 µg/ml Kevetrin for 6h and 6h plus 66h of wo, repeated for three times. Regarding phosphatidylserine externalization, in KASUMI-1 cell line, after the treatment, we observed an increase of Annexin V+ cells (early plus late apoptosis) compared to no drug control, not statistically significant. About MOLM-13 cell line we did not observe a significant variation of apoptotic cells percentage (Figure 12).

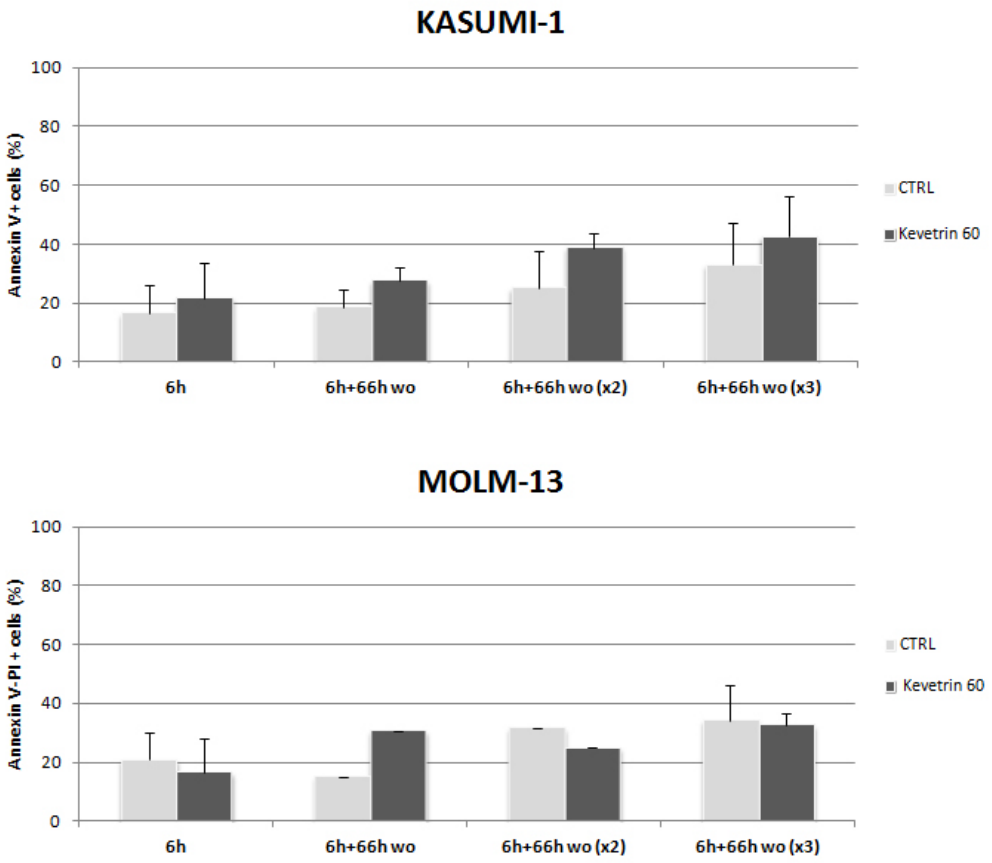

Figure 12. **Characterization of apoptosis induced by Kevetrin.**

Quantification of Annexin V+ cells in AML cell lines no drug and treated with Kevetrin at 60 µg/ml for 6h and 6h+66h wo (x1, x2, x3). Values represent the mean ± SD of three independent experiments.

Moreover, the data obtained were confirmed by TUNEL assay (Figure 13). We evaluated also the mitochondrial involvement and we didn't notice any alteration of mitochondrial membrane potential (data not shown).

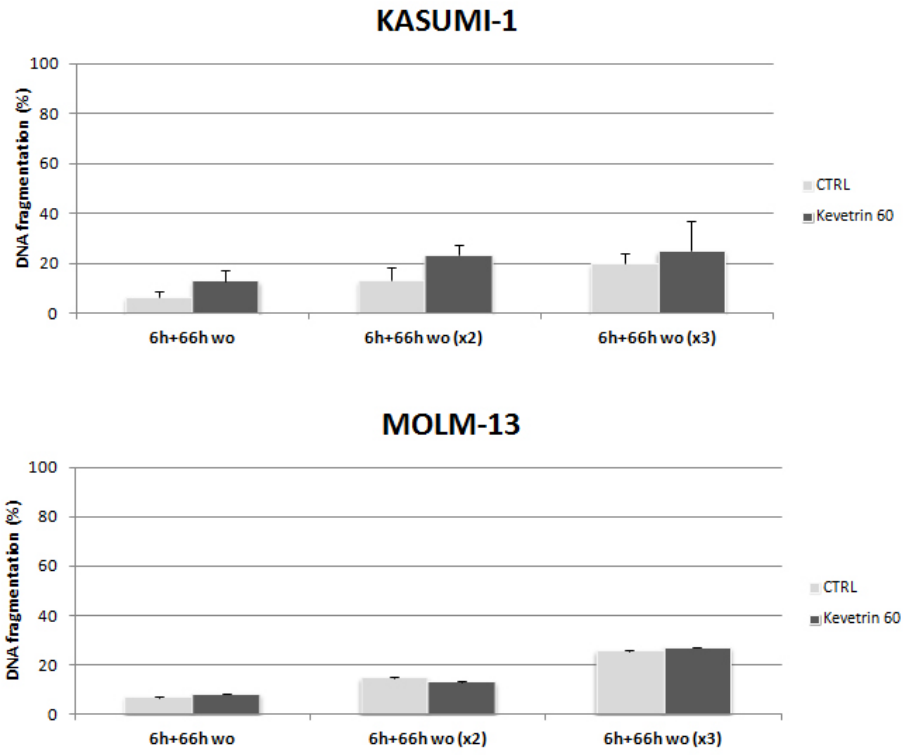

Figure 13. Evaluation of DNA fragmentation induced by Kevetrin in AML cell lines.

Percentage of DNA fragmentation in AML cell lines no drug controls and samples treated with Kevetrin at 60 µg/ml for 6h+66h wo (x1, x2, x3). Values represent the mean ± SD of three independent experiments.

3.3 REDUCED KEVETRIN TREATMENT TIME HAS A LOW EFFECT ON GENE EXPRESSION

We decided also to evaluate the effect of the treatment on gene expression regulation, performing a gene expression profiling (GEP) after 6h of treatment. In both the cell lines, after the treatment, we noticed an up-regulation of Metallothioneins in treated samples, compared to controls. The alterations were mainly associated to Metallothionein 1 isoform's subtypes and could be probably related to the oxidative stress induced by the treatment (Figure 14).

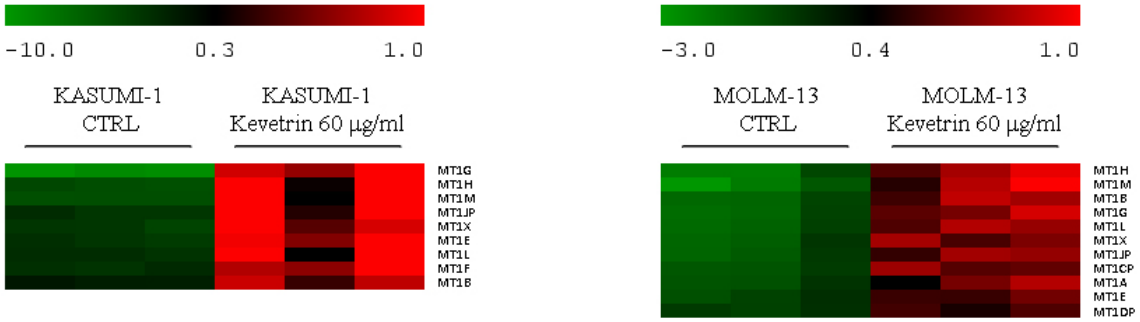

Figure 14. Gene expression profiling after 6h of treatment with Kevetrin.

Genes differentially expressed in AML cell lines controls and samples treated with Kevetrin at 60 µg/ml for 6h. Values are obtained from three independent experiments. Each row represents a gene and each column represents an independent experiment. The expression level of each gene is depicted according to a color scale shown at the top. Red and green indicate expression levels respectively above and below the median.

4. CONTINUED TREATMENT

Using a pulsed treatment we didn't understand clearly Kevetrin's mechanism of action in our models. We decided, indeed, to evaluate the effect of a continued treatment of 24 and 48 h.

4.1 KEVETRIN INDUCES A DECREASE OF VIABILITY IN AML CELL LINES

KASUMI-1 and MOLM-13 cell viability was evaluated using the MTS assay, after the exposure to different Kevetrin concentrations (15, 30 and 60 µg/ml) for 24, 48, and 72 h. As shown in Figure 15, the mutated cell line (KASUMI-1), presented a dose and time-dependent significant inhibition of cell viability, with IC50 at 48 h of treatment of 44.7 µg/ml.

The wild type cell line (MOLM-13), instead, presented a significant inhibition of cell viability only at the higher concentration (60 µg/ml), with an IC50 at 48 h of 57.8 µg/ml**.**
These data have demonstrated an anti-proliferative effect of Kevetrin, mostly on the mutated model, but also on the wild type one.

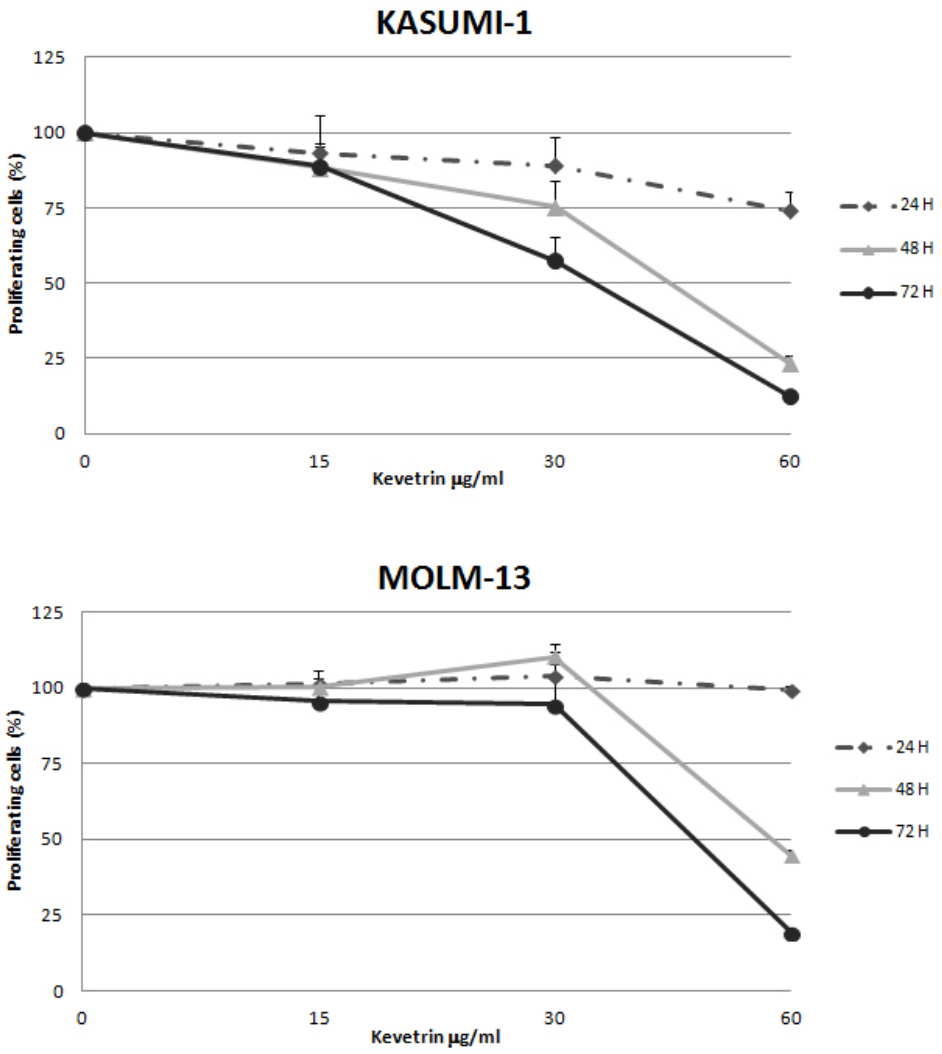

Figure 15. Kevetrin effect on AML cell lines proliferation.

Survival curve of AML cell lines treated with different concentrations of Kevetrin (15 – 30 – 60 µg/ml) for up to 72 h. Values represent the mean ± SD of three independent experiments in triplicate.

4.2 KEVETRIN INCREASES CELL SUSCEPTIBILITY TO APOPTOSIS

To investigate if apoptosis contributed to the anti-proliferative effect observed in AML cell lines, we examined phosphatidylserine externalization and DNA fragmentation after the treatment with Kevetrin at 15, 30 and 60 µg/ml for 24 and 48 h. As shown in Figure 16, in the mutated cell line (KASUMI-1) we observed an increase of Annexin V+ cells (early plus late apoptosis) in the treated samples compared to no drug control, statistically significant, at the higher concentration, after 24 h (38.35 ± 1.60 % vs 12.20 ± 2.54 %) and, extensively, after 48 h (17.30 ± 1.65 % for 15 µg/ml, 32.50 ± 0.60 % for 30 µg/ml and 79.70 ± 4.57 % for 60 µg/ml vs 13.18 ± 0.80 % for no drug control).

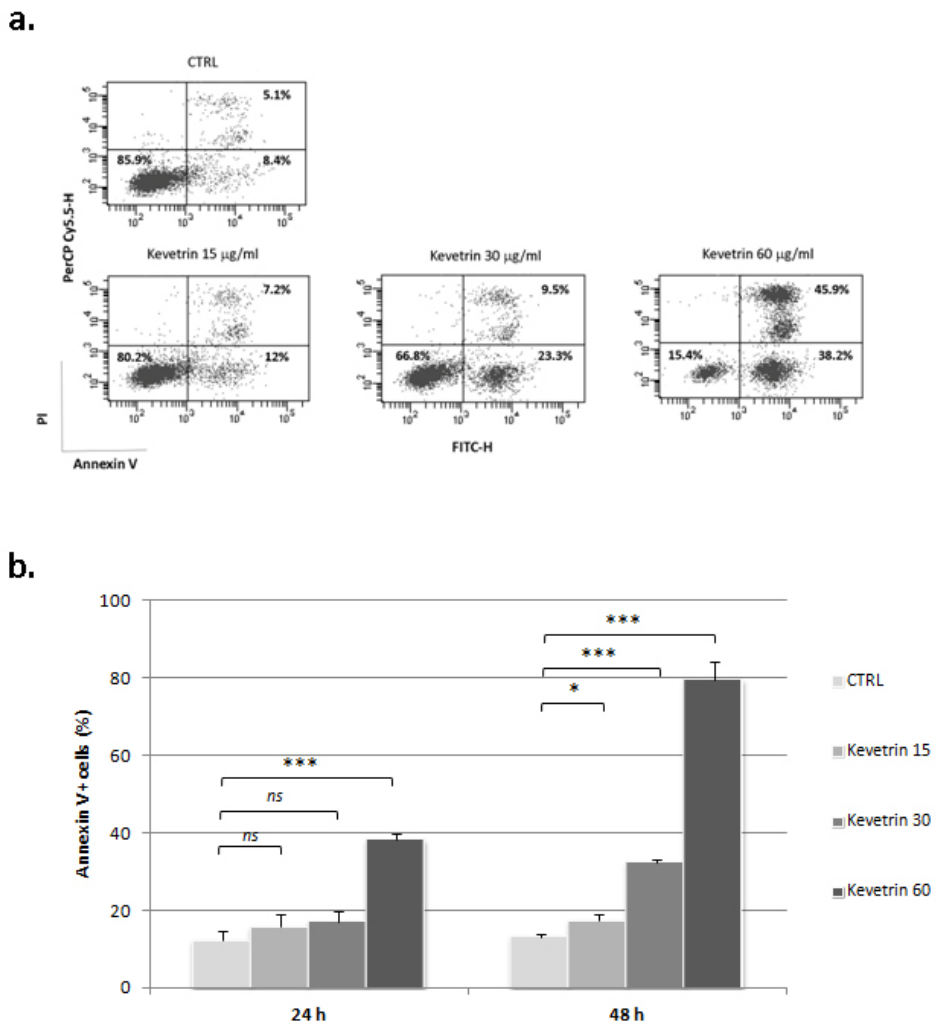

Figure 16. Characterization of apoptosis induced by Kevetrin in KASUMI-1 cell line.

(a) Representative dot plots of Annexin V – FITC and Propidium Iodide (PI) – PerCP Cy5.5 staining in KASUMI-1 cell line no drug and treated with Kevetrin at 15, 30 and 60 μg/ml for 48 h. (b) Quantification of Annexin V+ cells at 24 and 48 h. Values represent the mean ± SD of three independent experiments (*, P < 0.05, **, P < 0.005, ***, P < 0.0005 vs no drug; *ns*, not significant).

The presence of a great apoptosis induction was also confirmed by the statistically significant rise of DNA fragmentation (Figure 17 a), detected by Tunel assay, and by the great increment of Caspase-3 cleaved form (Figure 17 b). We also evaluated the cell cycle after 24 and 48 h of 60 μg/ml Kevetrin and we weren't able to describe cell cycle alterations due to the great apoptotic event (73.55 % vs 7.58 % of Apoptosis in no drug control) (Figure 17 c).

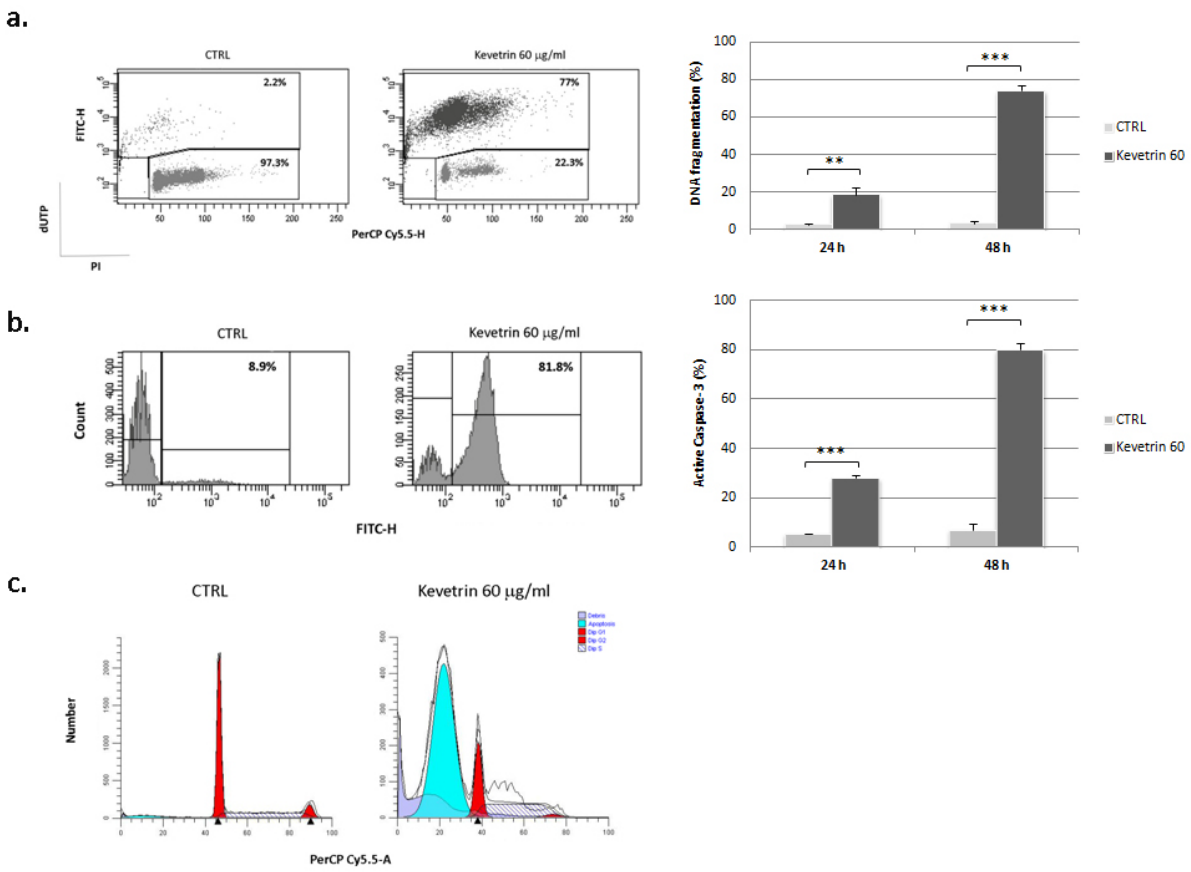

Figure 17. Evaluation of DNA fragmentation, Caspase-3 activation and Cell Cycle alterations induced by Kevetrin in KASUMI-1 cell line.

(a) Representative dot plots after 48 h and percentage of DNA fragmentation in KASUMI-1 cell line control and samples treated with Kevetrin 60 µg/ml for 24 and 48 h. (b) Representative cytofluorimetric histograms after 48 h and percentage of Active Caspase-3 in control and samples treated with Kevetrin 60 µg/ml for 24 and 48 h. (c) Representative histograms of cell cycle of control and sample treated with Kevetrin 60 µg/ml for 48 h. Values represent the mean ± SD of three independent experiments (*, P < 0.05, **, P < 0.005, ***, P < 0.0005 vs no drug; *ns*, not significant)

The wild type cell line (MOLM-13), in concordance with MTS data, showed a meaningful and statistically significant rise in apoptosis after 48 h at the concentration of 60 µg/ml, compared to no drug control, in terms of phosphatidylserine externalization (54.95 ± 5.63 % vs 12.53 ± 6.15 %)(Figure 18), DNA fragmentation (42.17 ± 5.27 % vs 1.97 ± 0.47 %)(Figure 19 a) and Caspase-3 activation (48.7 ± 7.21 % vs 5.7 ± 2.82 %)(Figure 19 b). No differences were observed at lower concentrations.

Also in this model we evaluated the cell cycle after 24 and 48 h of 60 µg/ml Kevetrin and we weren't able to point out cell cycle alterations due to the apoptosis increase (59.24 % vs 5.70 % of Apoptosis in no drug control) (Figure 19 c).

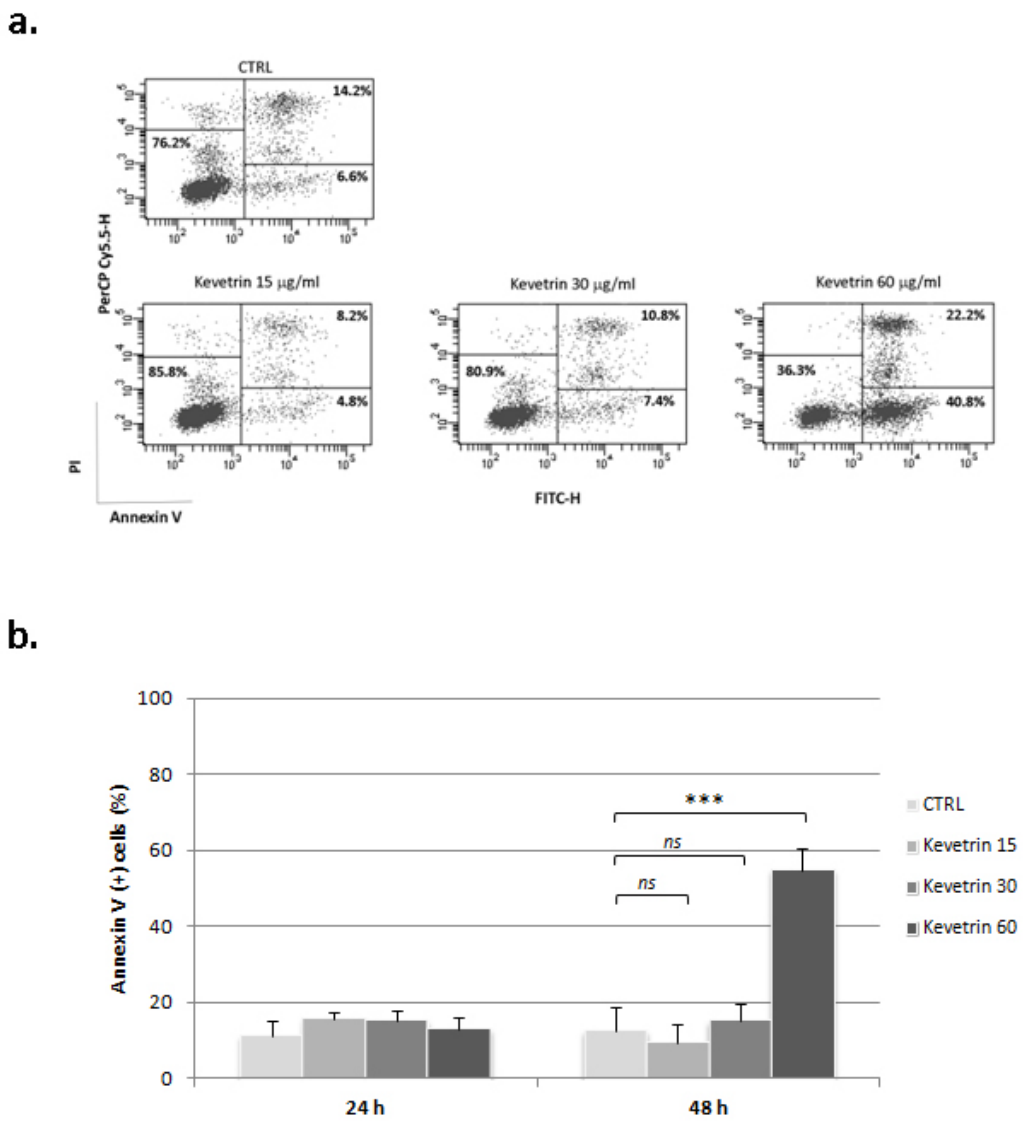

Figure 18. Characterization of apoptosis induced by Kevetrin in MOLM-13 cell line.

(a) Representative dot plots of Annexin V – FITC and Propidium Iodide (PI) – PerCP Cy5.5 staining in MOLM-13 cell line no drug and treated with Kevetrin at 15, 30 and 60 µg/ml for 48 h. (b) Quantification of Annexin V+ cells at 24 and 48 h. Values represent the mean ± SD of three independent experiments (*, P < 0.05, **, P < 0.005, ***, P < 0.0005 vs no drug; ns, not significant).

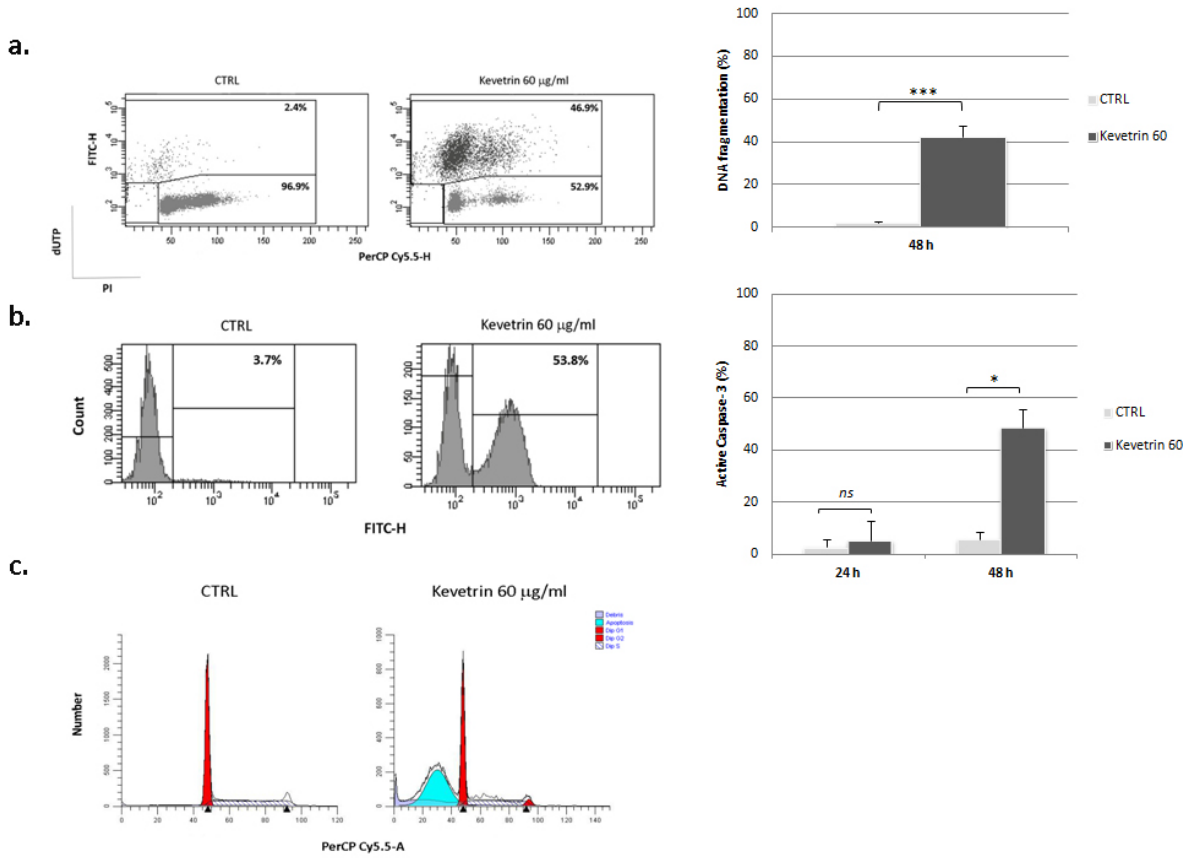

Figure 19. Evaluation of Evaluation of DNA fragmentation, Caspase-3 activation and Cell Cycle alterations induced in MOLM-13 cell line.

(a) Representative dot plots after 48 h and percentage of DNA fragmentation in MOLM-13 cell line control and samples treated with Kevetrin at 60 µg/ml for 24 and 48 h. (b) Representative cytofluorimetric histograms after 48 h and percentage of Active Caspase-3 in control and samples treated with Kevetrin at 60 µg/ml for 24 and 48 h. (c) Representative histograms of cell cycle alterations of control and sample treated 48 h with Kevetrin 60 µg/ml. Values represent the mean ± SD of three independent experiments (*, $P < 0.05$, **, $P < 0.005$, ***, $P < 0.0005$ vs no drug; *ns*, not significant).

4.3 KEVETRIN INDUCES MITOCHONDRIAL DEPOLARIZATION IN AML CELL LINES

In order to evaluate the mitochondrial involvement in the apoptotic process we decided to measure the mitochondrial membrane depolarization after 24 and 48 h of treatment. As shown in Figure 20 a, in KASUMI-1 cell line we observed, also in this case, a higher sensitivity, compared to the wild type model. More in details, in the mutated model Kevetrin exposure induced a rise of mitochondrial membrane depolarization in treated samples referred to no drug control, statistically significant at 60 µg/ml after 24 h (14.73 ± 0.89 % vs 5.40 ± 2.30 %) and also at lower concentrations, after a longer exposure (9.70 ± 1.70 % for 15 µg/ml, 20.97 ± 1.87 % for 30 µg/ml and 64.97 ± 4.29 % for 60 µg/ml vs 6.00 ± 0.72 % for no drug control, after 48 h).

Differently from KASUMI-1, MOLM-13 showed a statistically significant increase of mitochondrial membrane depolarization only after 48 h at 60 μg/ml, compared to no drug control (32.37 ± 7.73 % vs 3.87 ± 0.90 %) (Figure 20 b).

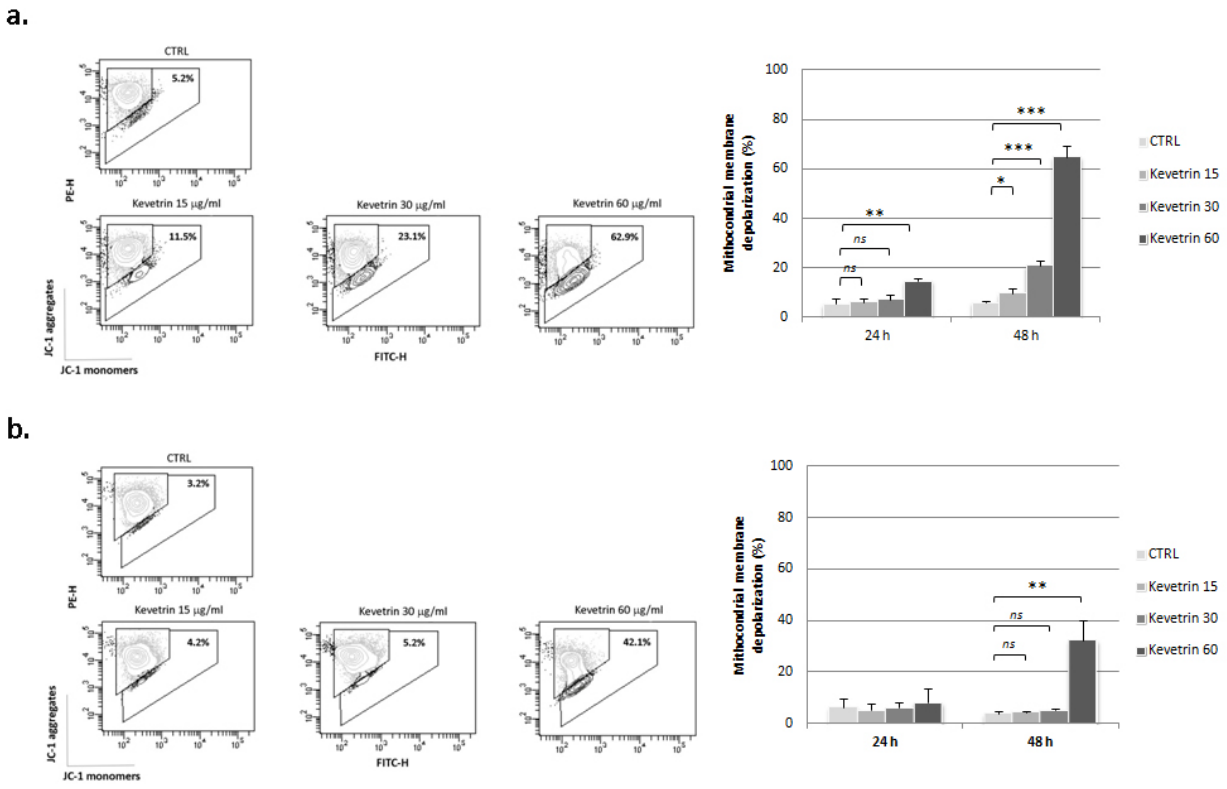

Figure 20. Kevetrin alters mitochondrial membrane potential in AML cell lines.

(a) Representative contour plots reporting the percentage of mitochondrial depolarization in controls and samples treated with Kevetrin at different concentrations (15 – 30 – 60 μg/ml) for 48 h and quantification of KASUMI-1 cells with depolarized mitochondria membrane after 24 and 48 h. (b) Representative contour plots reporting the percentage of mitochondrial depolarization for 48 h and quantification of MOLM-13 with depolarized mitochondria membrane after 24 and 48 h. Values represent the mean ± SD of three independent experiments (*, $p < 0.05$, **, $p < 0.005$, ***, $p < 0.0005$, *ns*, not significant).

4.4 KEVETRIN DIFFERENTLY AFFECTS THE EXPRESSION OF p53 AND ITS RELATED PROTEINS IN THE SELECTED MODELS

With the purpose to verify if the mechanism of action of our models was comparable to the one proposed by Cellceutix, we performed western blot analysis on both the cell lines, after 48 h of Kevetrin exposure at the concentrations of 15, 30 and 60 μg/ml. We identified a different mechanism of action for the mutated and the wild type model. In KASUMI-1 cell line the treatment induced a dose-dependent decrease of SIRT-3 expression, than the

relative untreated control. We also noticed a down-regulation of p53 total and active form (phosphorylated on Serine 15), more evident at the higher concentration, probably related also to the reduced expression of Hsp90; moreover we confirmed a reduced protein activity, examining two p53 substrates, PUMA and p21, that resulted less expressed after the treatment (Figure 21). The molecular effect in KASUMI-1 cell line wasn't dose-dependent, as the cellular one.

a.

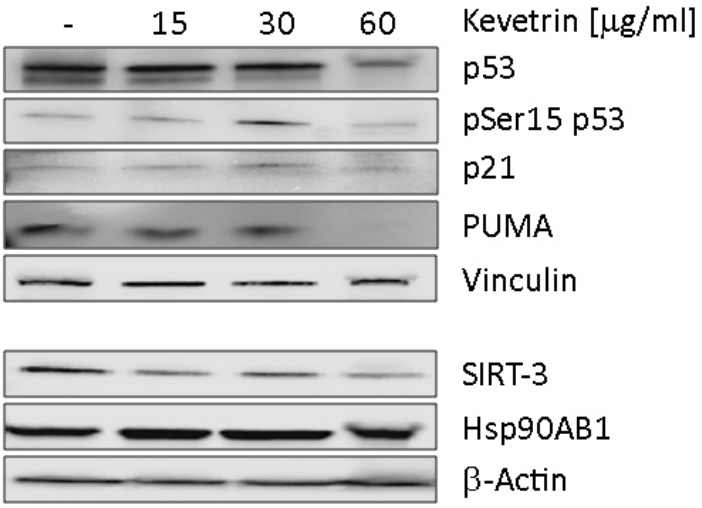

b.

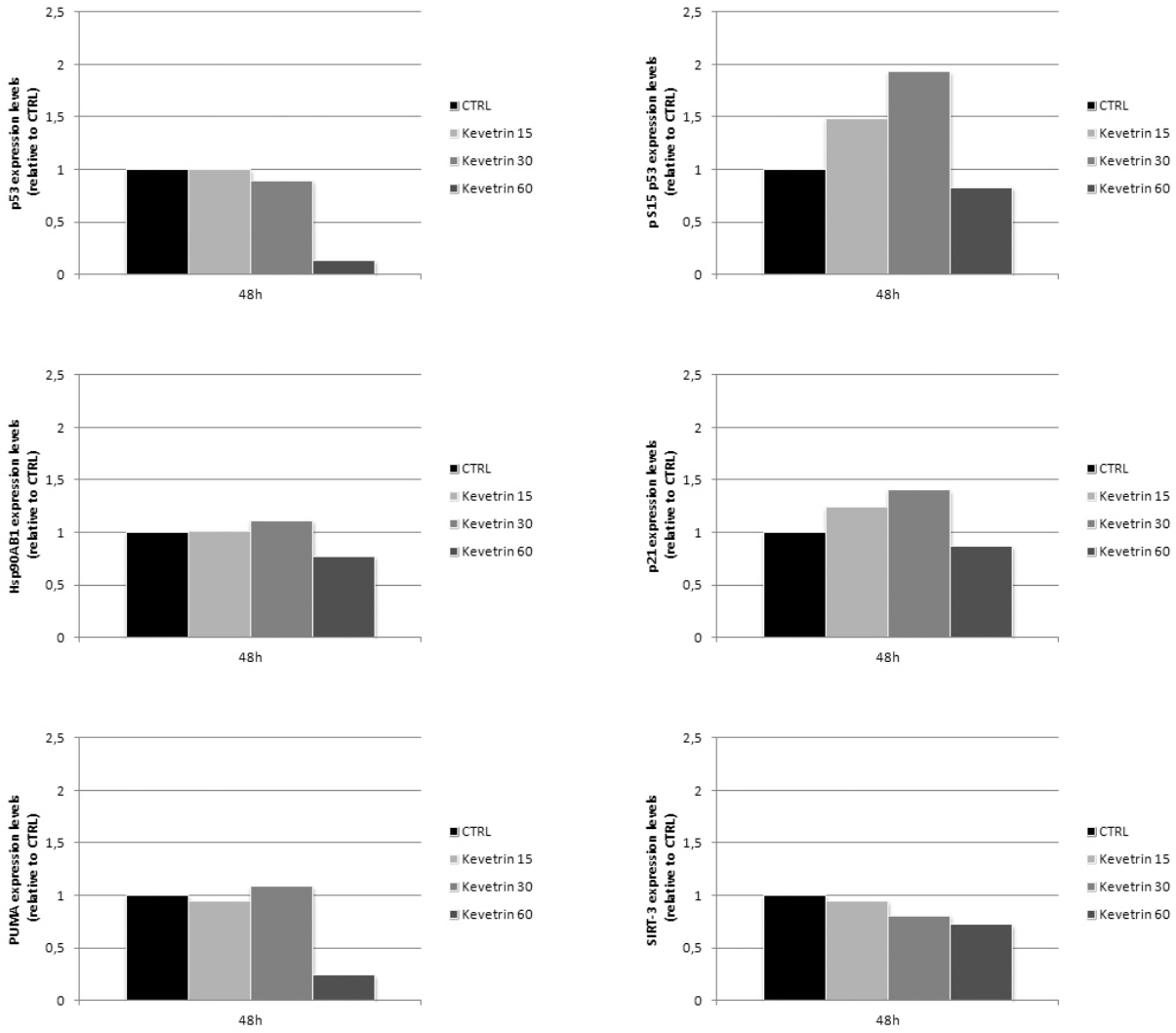

Figure 21. Kevetrin effect on the expression of p53 and its related proteins in KASUMI-1 cell line.

(a) Representative western blots of p53, pS15 p53, SIRT-3, PUMA, p21 and Hsp90 expression levels in KASUMI-1 cell line treated with Kevetrin at 15, 30 and 60 μg/ml for 48 h. β-actin and vinculin were used as loading control. (b) Relative densitometric analysis in KASUMI-1 cell line treated with Kevetrin at the above concentrations.

In MOLM-13, the scenario was quite different: we noticed, unequally from the described non-hematological wild type models, a down-regulation of total p53 and a stable expression of its active form (pS15 p53), in treated samples referred to no drug controls. Evaluating p53 target proteins we found a reduced expression of PUMA but a great up-regulation of p21, more evident at the higher concentration. We also found a reduction of Hsp90 and a rise in SIRT-3 expression (Figure 22).

a.

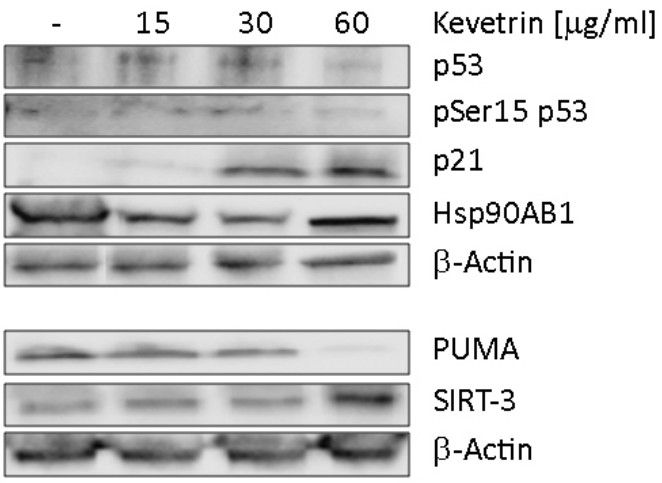

b.

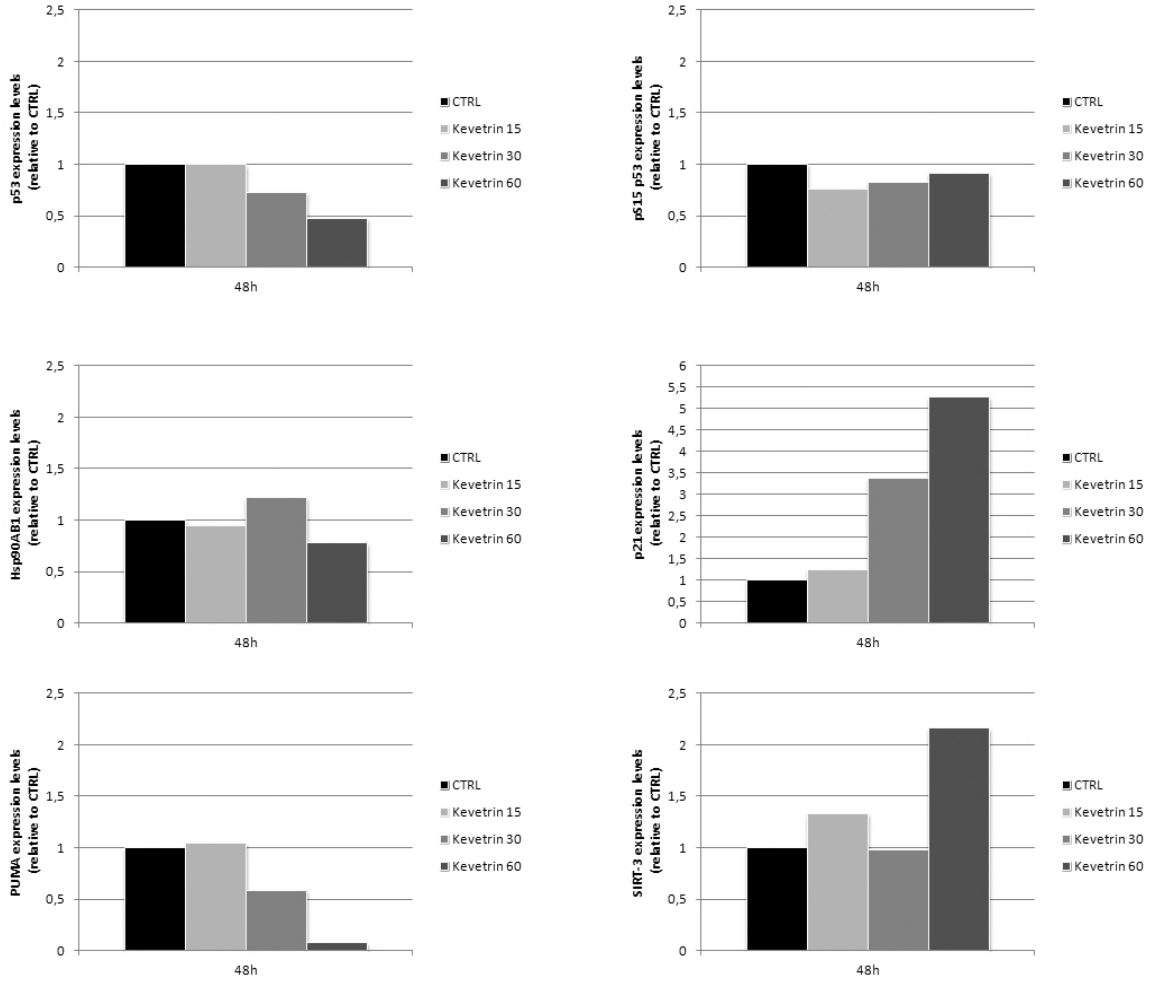

Figure 22. Kevetrin effect on the expression of p53 and its related proteins in MOLM-13 cell line.

(a) Representative western blots of p53, p53(Ser15), SIRT-3, PUMA, p21 and Hsp90 expression levels in MOLM-13 cell line treated with Kevetrin at 15, 30 and 60 μg/ml for 48 h. β-actin was used as loading control. (b) Relative densitometric analysis in MOLM-13 cell line treated with Kevetrin at the above concentrations.

4.5 KEVETRIN ALTERS THE LOCALIZATION OF p53 IN AML CELL LINES

With the purpose to verify if the p53 down-regulation was also associated to a different protein localization, we performed immunofluorescence analysis, after 24 and 48 h at the concentration of 60 μg/ml Kevetrin.

In KASUMI-1 cell line the treatment induced a cytoplasmic localization, more evident after 48 h, if compared to the nuclear localization of the relative control.

In the wild type model (MOLM-13) we did not observe any alteration after 24 h and, also in this case, we found a more p53 cytoplasmic localization after 48 h of treatment with 60 μg/ml Kevetrin (Figure 23).

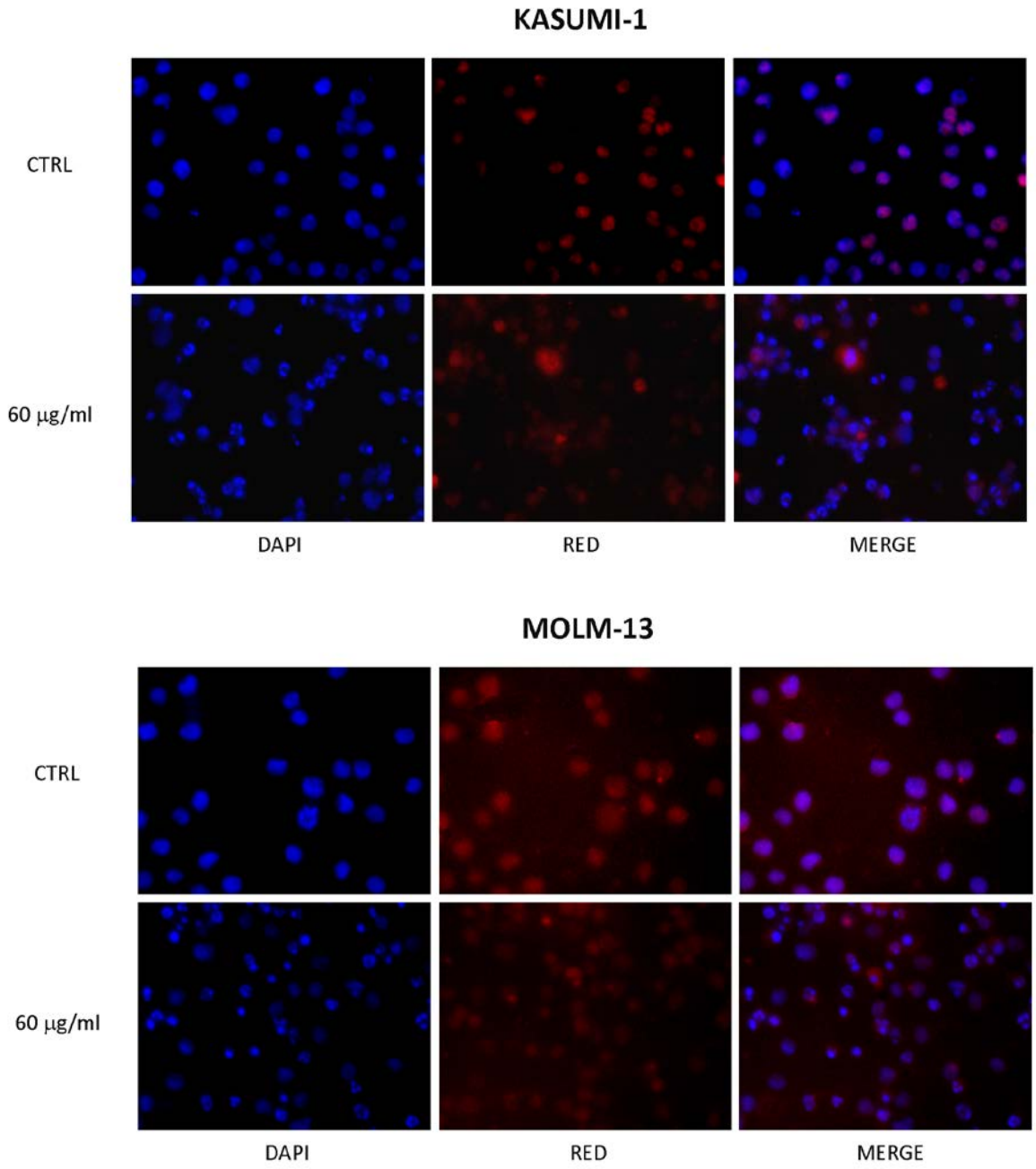

Figure 23. Expression of p53 in KASUMI-1 and MOLM-13 cell lines.

P53 protein expression before (CTRL) and after 48 h of treatment with Kevetrin 60 μg/ml. Nuclei are stained with DAPI (DAPI= 4'-6-Diamidino-2-phenylindole), while p53 is detected through a monoclonal antibody (red signal). Co-localization of nuclei and p53 is presented in violet in the merged image. Images are acquired using a 20x objective.

DISCUSSION

Acute Myeloid Leukemia (AML) is a clonal disorder defined by myeloid progenitors expansion and proliferation. AML therapeutic strategy over the past 30 years hasn't been changed and, nowadays AML is curable in the most of patients younger than 60 years old. For those older than 60 the prognosis remains unhappy (1)(2). Tumor suppressor p53 is a fundamental regulator of several responses associated to stress signals, such as DNA damage, hypoxia and hyperproliferation, modulating numerous genes with a key role in cell-cycle arrest and DNA repair (27). *TP53* is one of the most mutated gene in human tumors (54). The frequency of *TP53* gene mutation in AML patients is approximately 8%, and those mutations are predominantly associated with complex aberrant karyotype, conferring a very poor outcome (2)(17).

The novel Cellceutix's nitrile derivative, Kevetrin, has showed a great activity in several solid tumors, presenting a different mechanism of action for wild type and mutated *TP53* models. Geoffrey S. and colleagues reported, indeed, a remarkable role of Kevetrin in promoting p53 wild type activity restoration, inducing apoptosis through the increased expression of p53 target genes, *p21* and *PUMA* (45). Regarding *TP53* mutated models, the pro-apoptotic activity of this new compound can be due to the dissociation of the Hsp90-p53 oncogenic complex that allows the mutated form's degradation (50).

In the present study we evaluated if Kevetrin could be active also on hematological models, testing the drug on AML cell lines. Starting from a schedule more close to the clinical protocol, we tested a pulsed treatment that showed a particular sensitivity of the mutated cell line (KASUMI-1), associated to a great growth arrest but a less marked apoptosis induction. A different effect was observed on the wild type cell line (MOLM-13), that was more resistant to the treatment.

Using a continue treatment schedule, we observed a more evident effect. Our data indicate that Kevetrin exposure induces cell growth arrest, a great drop of mitochondrial membrane potential and a remarkable increment of Caspase-3 cleaved form, features that contribute to apoptotic cell death in the two cell lines. Cellular effects can be associated with a dose and time-dependent effect in KASUMI-1 cell line but not in MOLM-13, in which we can observe an activity only at the higher concentration, after 48 h.

We decided to clarify Kevetrin's mechanism of action in the two cell lines, verifying if the effect of the molecule was related to p53, as observed by Cellceutix in solid cancer models (45)(50).

At first we evaluated the expression of p53 in its total and active form, phosphorylated on Serine 15, a modification that occurs after DNA damage for reducing p53-MDM2 interaction and promoting increased levels of transcriptionally active p53 (36). After 48 h of Kevetrin 60 μg/ml exposure in KASUMI-1 cell line we found a great p53 down-regulation, also confirmed by a different localization of the protein, more nuclear in no drug control and cytoplasmic in the treated sample, suggesting an increased proteasomal degradation. In concordance with the mechanism of action proposed by Cellceutix, in our model p53 reduced expression could be due to Hsp90 down-regulation, resulting in a less marked formation of the Hsp90-p53 oncogenic complex, with an increased protein degradation. Several studies, indeed, underlined a higher interaction of mutated p53 to Hsp90, compared to the wild type protein (55)(56) and how chaperon function's inhibition can promote mutant p53 degradation (57). We also found a down-regulated p53 active form, associated to a more reduced expression of p53 target proteins, such as p21 and PUMA. Moreover, we found a down-regulation of SIRT-3 protein expression (Figure 24).

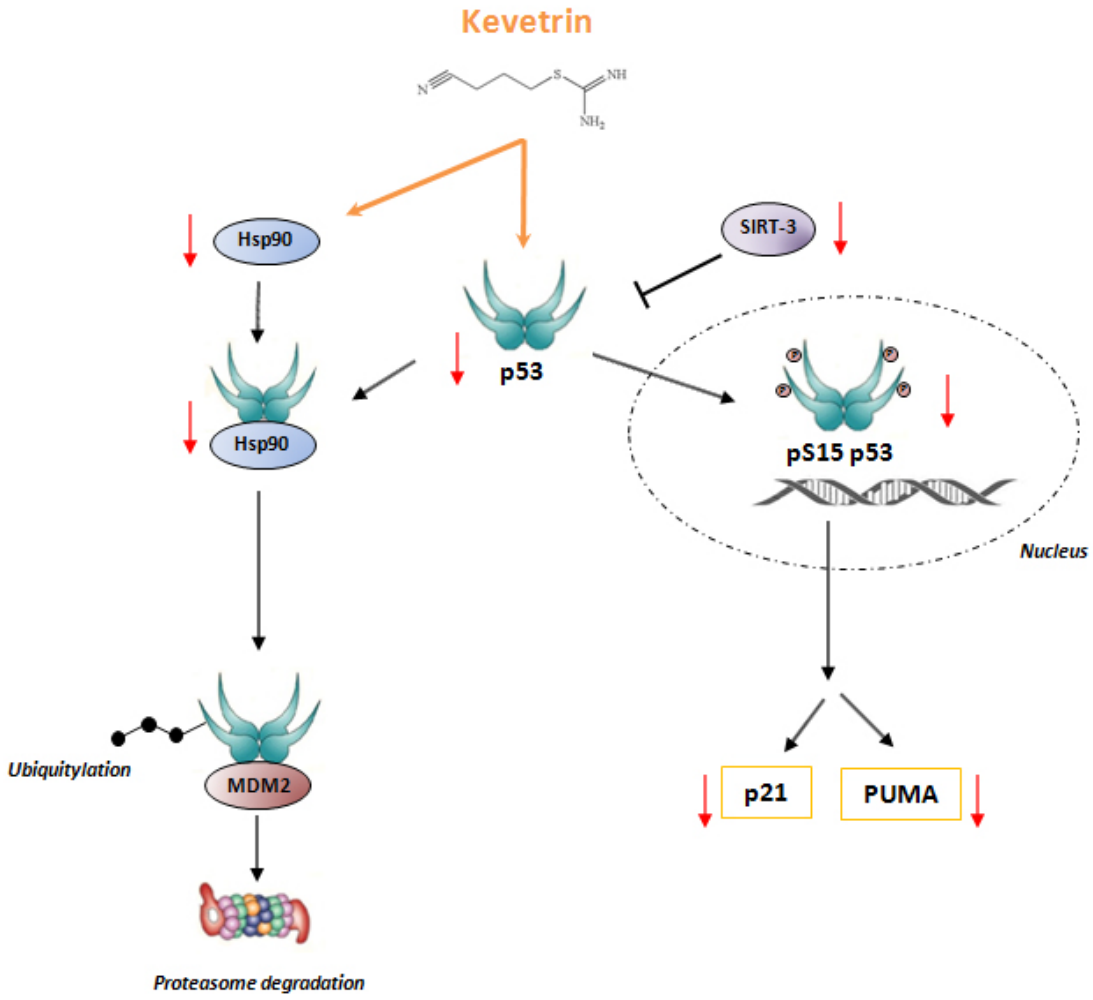

Figure 24. Kevetrin's mechanism of action in KASUMI-1 cell line.

Considering MOLM-13 cell line, after 48 h of treatment with Kevetrin 60 µg/ml we found, differently from solid cancer models, a great p53 down-regulation, confirmed by a more cytoplasmic protein localization after the treatment, compared to no drug control. p53 reduced expression could be also due to SIRT-3 up-regulation and Hsp90 down-regulation. SIRT-3, indeed, exert an inhibitory activity on total p53, as reported by Li S. *et al.* (40), and Hsp90 has been proved to be fundamental for the stability and the DNA binding capacity of the wild type protein (58)(59). Regarding p53 active form, phosphorylated on Serine 15, we noticed slight variations in protein expression, if compared to the great p53 down-regulation, suggesting a physiological response of the protein to the cellular damage. In accordance with p53 activity, we observed a great up-regulation of p21, promoting cell cycle arrest, probably associated with a drug resistance mechanism. In contrast, PUMA protein was highly down-regulated, suggesting a p53-independent mechanism of action (60) or a feedback regulation of the apoptotic process, after Caspase-3 activation (61) (Figure 25).

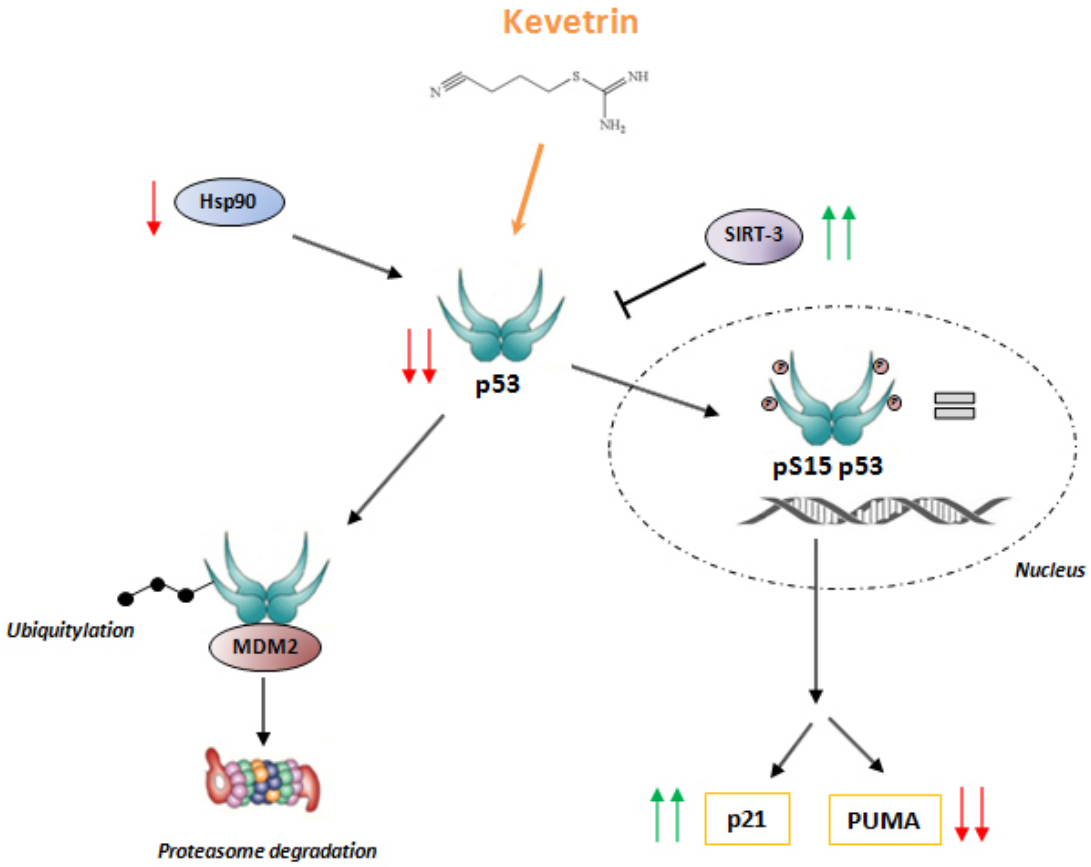

Figure 25. Kevetrin's mechanism of action in MOLM-13 cell line.

This last aspect will be subject to further research in order to ameliorate our understanding of Kevetrin's mechanism of action in the two cell lines. In this regard we are actually performing gene expression profiling after 48 h of treatment with Kevetrin 60 μg/ml on both the cell lines.

Our results suggest that Kevetrin may represent a promising drug in AML patients treatment, both in wild type and even more in *TP53* mutated tumors, through different molecular mechanisms, giving more therapeutic alternatives in the treatment of this disease.

BIBLIOGRAPHY

(1) Saultz JN, Garzon R. Acute Myeloid Leukemia: A Concise Review. J Clin Med 2016 Mar 5;5(3):10.3390/jcm5030033.

(2) Dohner H, Weisdorf DJ, Bloomfield CD. Acute Myeloid Leukemia. N Engl J Med 2015 Sep 17;373(12):1136-1152.

(3) Estey E, Dohner H. Acute myeloid leukaemia. Lancet 2006 Nov 25;368(9550):1894-1907.

(4) Dohner H, Estey E, Grimwade D, Amadori S, Appelbaum FR, Buchner T, et al. Diagnosis and management of AML in adults: 2017 ELN recommendations from an international expert panel. Blood 2016 Nov 28.

(5) Bennett JM, Catovsky D, Daniel MT, Flandrin G, Galton DA, Gralnick HR, et al. Proposals for the classification of the acute leukaemias. French-American-British (FAB) co-operative group. Br J Haematol 1976 Aug;33(4):451-458.

(6) Tenen DG. Disruption of differentiation in human cancer: AML shows the way. Nat Rev Cancer 2003 Feb;3(2):89-101.

(7) Campos L, Guyotat D, Archimbaud E, Devaux Y, Treille D, Larese A, et al. Surface marker expression in adult acute myeloid leukaemia: correlations with initial characteristics, morphology and response to therapy. Br J Haematol 1989 Jun;72(2):161-166.

(8) Wolach O, Stone RM. How I treat mixed-phenotype acute leukemia. Blood 2015 Apr 16;125(16):2477-2485.

(9) Ladines-Castro W, Barragán-Ibanez G, Luna-Pérez MA, Santoyo-Sánchez A, Collazo-Jaloma J, Mendoza-García E, et al. Morphology of leukaemias. Revista Médica del Hospital General de México 2016;79(2):107-113.

(10) Byrd JC, Mrozek K, Dodge RK, Carroll AJ, Edwards CG, Arthur DC, et al. Pretreatment cytogenetic abnormalities are predictive of induction success, cumulative incidence of relapse, and overall survival in adult patients with de novo acute myeloid leukemia: results from Cancer and Leukemia Group B (CALGB 8461). Blood 2002 Dec 15;100(13):4325-4336.

(11) Cancer Genome Atlas Research Network. Genomic and epigenomic landscapes of adult de novo acute myeloid leukemia. N Engl J Med 2013 May 30;368(22):2059-2074.

(12) Kelly LM, Liu Q, Kutok JL, Williams IR, Boulton CL, Gilliland DG. FLT3 internal tandem duplication mutations associated with human acute myeloid leukemias induce myeloproliferative disease in a murine bone marrow transplant model. Blood 2002 Jan 1;99(1):310-318.

(13) Kayser S, Schlenk RF, Londono MC, Breitenbuecher F, Wittke K, Du J, et al. Insertion of FLT3 internal tandem duplication in the tyrosine kinase domain-1 is associated with resistance to chemotherapy and inferior outcome. Blood 2009 Sep 17;114(12):2386-2392.

(14) Tang JL, Hou HA, Chen CY, Liu CY, Chou WC, Tseng MH, et al. AML1/RUNX1 mutations in 470 adult patients with de novo acute myeloid leukemia: prognostic implication and interaction with other gene alterations. Blood 2009 Dec 17;114(26):5352-5361.

(15) Falini B, Nicoletti I, Martelli MF, Mecucci C. Acute myeloid leukemia carrying cytoplasmic/mutated nucleophosmin (NPMc+ AML): biologic and clinical features. Blood 2007 Feb 1;109(3):874-885.

(16) Lindsley RC, Mar BG, Mazzola E, Grauman PV, Shareef S, Allen SL, et al. Acute myeloid leukemia ontogeny is defined by distinct somatic mutations. Blood 2015 Feb 26;125(9):1367-1376.

(17) Haferlach C, Dicker F, Herholz H, Schnittger S, Kern W, Haferlach T. Mutations of the TP53 gene in acute myeloid leukemia are strongly associated with a complex aberrant karyotype. Leukemia 2008 Aug;22(8):1539-1541.

(18) Wang ZY, Chen Z. Acute promyelocytic leukemia: from highly fatal to highly curable. Blood 2008 Mar 1;111(5):2505-2515.

(19) Mrozek K, Marcucci G, Nicolet D, Maharry KS, Becker H, Whitman SP, et al. Prognostic significance of the European LeukemiaNet standardized system for reporting cytogenetic and molecular alterations in adults with acute myeloid leukemia. J Clin Oncol 2012 Dec 20;30(36):4515-4523.

(20) Wander SA, Levis MJ, Fathi AT. The evolving role of FLT3 inhibitors in acute myeloid leukemia: quizartinib and beyond. Ther Adv Hematol 2014 Jun;5(3):65-77.

(21) Wang F, Travins J, DeLaBarre B, Penard-Lacronique V, Schalm S, Hansen E, et al. Targeted inhibition of mutant IDH2 in leukemia cells induces cellular differentiation. Science 2013 May 3;340(6132):622-626.

(22) Issa JP, Roboz G, Rizzieri D, Jabbour E, Stock W, O'Connell C, et al. Safety and tolerability of guadecitabine (SGI-110) in patients with myelodysplastic syndrome and acute myeloid leukaemia: a multicentre, randomised, dose-escalation phase 1 study. Lancet Oncol 2015 Sep;16(9):1099-1110.

(23) Gasiorowski RE, Clark GJ, Bradstock K, Hart DN. Antibody therapy for acute myeloid leukaemia. Br J Haematol 2014 Feb;164(4):481-495.

(24) Brosh R, Rotter V. When mutants gain new powers: news from the mutant p53 field. Nat Rev Cancer 2009 Oct;9(10):701-713.

(25) Pessòa I.A., P. Estumano da Silva, F., Praia Anselmo N, C. de Oliveira E.H. Alterations in TP53 gene – Implications in Tumorigenesis Process and Prognosis in Central Nervous System Cancer. Tumors of the Central Nervous System - Primary and Secondary: Dr. Lee Roy Morgan; 2014.

(26) Hollstein M, Sidransky D, Vogelstein B, Harris CC. P53 Mutations in Human Cancers. Science 1991 Jul 5;253(5015):49-53.

(27) Scoumanne A, Chen X. Protein methylation: a new mechanism of p53 tumor suppressor regulation. Histol Histopathol 2008 Sep;23(9):1143-1149.

(28) Harms K, Nozell S, Chen X. The common and distinct target genes of the p53 family transcription factors. Cell Mol Life Sci 2004 Apr;61(7-8):822-842.

(29) Helton ES, Chen X. p53 modulation of the DNA damage response. J Cell Biochem 2007 Mar 1;100(4):883-896.

(30) Hagn F, Lagleder S, Retzlaff M, Rohrberg J, Demmer O, Richter K, et al. Structural analysis of the interaction between Hsp90 and the tumor suppressor protein p53. Nat Struct Mol Biol 2011 Sep 4;18(10):1086-1093.

(31) Honda R, Tanaka H, Yasuda H. Oncoprotein MDM2 is a ubiquitin ligase E3 for tumor suppressor p53. FEBS Lett 1997 Dec 22;420(1):25-27.

(32) Haupt Y, Maya R, Kazaz A, Oren M. Mdm2 promotes the rapid degradation of p53. Nature 1997 May 15;387(6630):296-299.

(33) Oliner JD, Pietenpol JA, Thiagalingam S, Gyuris J, Kinzler KW, Vogelstein B. Oncoprotein MDM2 conceals the activation domain of tumour suppressor p53. Nature 1993 Apr 29;362(6423):857-860.

(34) Chen J, Lin J, Levine AJ. Regulation of transcription functions of the p53 tumor suppressor by the mdm-2 oncogene. Mol Med 1995 Jan;1(2):142-152.

(35) Bakkenist CJ, Kastan MB. Initiating cellular stress responses. Cell 2004 Jul 9;118(1):9-17.

(36) Lakin ND, Jackson SP. Regulation of p53 in response to DNA damage. Oncogene 1999 Dec 13;18(53):7644-7655.

(37) Bullock AN, Fersht AR. Rescuing the function of mutant p53. Nat Rev Cancer 2001 Oct;1(1):68-76.

(38) Bieging KT, Mello SS, Attardi LD. Unravelling mechanisms of p53-mediated tumour suppression. Nat Rev Cancer 2014 May;14(5):359-370.

(39) Chen Y, Fu LL, Wen X, Wang XY, Liu J, Cheng Y, et al. Sirtuin-3 (SIRT3), a therapeutic target with oncogenic and tumor-suppressive function in cancer. Cell Death Dis 2014 Feb 6;5:e1047.

(40) Li S, Banck M, Mujtaba S, Zhou MM, Sugrue MM, Walsh MJ. p53-induced growth arrest is regulated by the mitochondrial SirT3 deacetylase. PLoS One 2010 May 5;5(5):e10486.

(41) Menon K. Nitrile derivatives and their pharmaceutical use and compositions. 2012 dec # 25.

(42) Banu N, Hiran T, Chafai-Fadela K, Menon KE. AKT inhibitor has potent antitumor activity in human lung cancer xenograft models. Cancer research 2009;69(23; supplement).

(43) Ashbaugh E, Morello M. Kevetrin: a novel genetic cancer treatment. University of Pittsburgh, Swanson School of Engineering 2013.

(44) Cellceutix. 2016; Available at: http://www.cellceutix.com/.

(45) Kumar A, Hiran T, Holden SA, Chafai-Fadela K, Rogers S, Ram S, et al. Kevetrin™, a novel small molecule, activates p53, enhances expression of p21, induces cell cycle arrest and apoptosis in a human cancer cell line. Cancer research 2011;71(8; supplement).

(46) Cheung CH, Chen HH, Cheng LT, Lyu KW, Kanwar JR, Chang JY. Targeting Hsp90 with small molecule inhibitors induces the over-expression of the anti-apoptotic molecule,

survivin, in human A549, HONE-1 and HT-29 cancer cells. Mol Cancer 2010 Apr 15;9:77-4598-9-77.

(47) Dempsey NC, Leoni F, Ireland HE, Hoyle C, Williams JH. Differential heat shock protein localization in chronic lymphocytic leukemia. J Leukoc Biol 2010 Mar;87(3):467-476.

(48) Mjahed H, Girodon F, Fontenay M, Garrido C. Heat shock proteins in hematopoietic malignancies. Exp Cell Res 2012 Sep 10;318(15):1946-1958.

(49) Flandrin P, Guyotat D, Duval A, Cornillon J, Tavernier E, Nadal N, et al. Significance of heat-shock protein (HSP) 90 expression in acute myeloid leukemia cells. Cell Stress Chaperones 2008 Sep;13(3):357-364.

(50) Kumar A, Holden SA, Chafai-Fadela K, Ram S, Menon KE. Kevetrin targets both MDM2-p53 and Rb-E2F pathways in tumor suppression. Cancer research 2012;72(8; supplement).

(51) Shapiro G, G. Supko J, C. Cho D, Hilton JF, Hadfield M, Pruitt-Thompson S, et al. A phase I, dose-escalation, safety, pharmacokinetic, pharmacodynamic study of thioureidobutyronitrile, a novel p53 targeted therapy, in patients with advanced solid tumors. Journal of clinical oncology : official journal of the American Society of Clinical Oncology 2013;31(suppl; abstr TPS2627).

(52) Shapiro G, Mier JW, Hilton JF, Gandhi L, G. Chau N, J. Bullock A, et al. A phase 1, dose-escalation, safety, pharmacokinetic, pharmacodynamic study of thioureidobutyronitrile, a novel p53 targeted therapy, in patients with advanced solid tumors. Journal of clinical oncology : official journal of the American Society of Clinical Oncology 2015;33(suppl; abstr TPS2613).

(53) Nag S, Qin J, Srivenugopal KS, Wang M, Zhang R. The MDM2-p53 pathway revisited. J Biomed Res 2013 Jul;27(4):254-271.

(54) Kandoth C, McLellan MD, Vandin F, Ye K, Niu B, Lu C, et al. Mutational landscape and significance across 12 major cancer types. Nature 2013 Oct 17;502(7471):333-339.

(55) Blagosklonny MV, Toretsky J, Bohen S, Neckers L. Mutant conformation of p53 translated in vitro or in vivo requires functional HSP90. Proc Natl Acad Sci U S A 1996 Aug 6;93(16):8379-8383.

(56) Whitesell L, Sutphin PD, Pulcini EJ, Martinez JD, Cook PH. The physical association of multiple molecular chaperone proteins with mutant p53 is altered by geldanamycin, an hsp90-binding agent. Mol Cell Biol 1998 Mar;18(3):1517-1524.

(57) Peng Y, Chen L, Li C, Lu W, Chen J. Inhibition of MDM2 by hsp90 contributes to mutant p53 stabilization. J Biol Chem 2001 Nov 2;276(44):40583-40590.

(58) Muller L, Schaupp A, Walerych D, Wegele H, Buchner J. Hsp90 regulates the activity of wild type p53 under physiological and elevated temperatures. J Biol Chem 2004 Nov 19;279(47):48846-48854.

(59) Whitesell L, Lindquist SL. HSP90 and the chaperoning of cancer. Nat Rev Cancer 2005 Oct;5(10):761-772.

(60) Yu J, Zhang L. PUMA, a potent killer with or without p53. Oncogene 2008 Dec;27 Suppl 1:S71-83.

(61) Hadji A, Clybouw C, Auffredou MT, Alexia C, Poalas K, Burlion A, et al. Caspase-3 triggers a TPCK-sensitive protease pathway leading to degradation of the BH3-only protein puma. Apoptosis 2010 Dec;15(12):1529-1539.

ATTACHMENT

During my PhD I've also collaborated into several research projects producing the articles mentioned below:

1) **Project:**
   Investigation of functional alteration in T cells from patients with Acute Myeloid Leukemia (AML) and *in vitro* reactivation of subpopulations of the immune system induced by immunomodulatory agents

   Articles:
   Musuraca G, De Matteis S, **Napolitano R**, Papayannidis C, Guadagnuolo V, Fabbri F, Cangini D, Ceccolini M, Giannini MB, Lucchesi A, Ronconi S, Mariotti P, Savini P, Tani M, Fattori PP, Guidoboni M, Martinelli G, Zoli W, Amadori D, Carloni S. IL-17/IL-10 double-producing T cells: new link between infections, immunosuppression and acute myeloid leukemia. J Transl Med. 2015 Jul 15;13:229.

2) **Project:**
   Analysis and role of GSK3beta and HINT1 in the pathogenesis and therapy responsiveness of classical Hodgkin Lymphoma patients.

   Articles:
   Vergara D, Simeone P, De Matteis S, Carloni S, Lanuti P, Marchisio M, Miscia S, Rizzello A, **Napolitano R**, Agostinelli C, Maffia M. Comparative proteomic profiling of Hodgkin lymphoma cell lines. Mol Biosyst. 2016 Jan;12(1):219-32.

   Agostinelli C, Carloni S, Limarzi F, Righi S, Laginestra MA, Musuraca G, Fiorentino M, **Napolitano R**, **Cuneo A**, Vergara D, Zinzani PL, Elena S, Pileri SA, De Matteis S. Emerging role of GSK-3β in the pathobiology of classical Hodgkin Lymphoma. Histopatology. 2017 Feb 16.